385

CONFIDENTIAL

Superseded by TND-893

NACA

RESEARCH MEMORANDUM

PRESSURE LOADS PRODUCED ON A FLAT-PLATE WING BY ROCKET

JETS EXHAUSTING IN A SPANWISE DIRECTION BELOW THE

WING AND PERPENDICULAR TO A FREE-STREAM

FLOW OF MACH NUMBER 2.0

By Ralph A. Falanga and Joseph J. Janos

Langley Aeronautical Laboratory
Langley Field, Va.

Classification Changed to Unclassified
Authority: NASA Technical Publications
Announcements No. 33
Effective Date: October 28, 1960
WHL

NATIONAL ADVISORY COMMITTEE
FOR AERONAUTICS

WASHINGTON

June 5, 1958

CONFIDENTIAL

CONFIDENTIAL

NATIONAL ADVISORY COMMITTEE FOR AERONAUTICS

RESEARCH MEMORANDUM

PRESSURE LOADS PRODUCED ON A FLAT-PLATE WING BY ROCKET

JETS EXHAUSTING IN A SPANWISE DIRECTION BELOW THE

WING AND PERPENDICULAR TO A FREE-STREAM

FLOW OF MACH NUMBER 2.0

By Ralph A. Falanga and Joseph J. Janos

SUMMARY

An investigation at a Reynolds number per foot of 14.4×10^6 was made to determine the pressure loads produced on a flat-plate wing by rocket jets exhausting in a spanwise direction beneath the wing and perpendicular to a free-stream flow of Mach number 2.0. The ranges of the variables involved were (1) nozzle types - one sonic (jet Mach number of 1.00), two supersonic (jet Mach numbers of 1.74 and 3.04), and one two-dimensional supersonic (jet Mach number of 1.71); (2) vertical nozzle positions beneath the wing of 4, 8, and 12 nozzle-throat diameters; and (3) ratios of rocket-chamber total pressure to free-stream static pressure from 0 to 130.

The incremental normal force due to jet interference on the wing varied from one to two times the rocket thrust and generally decreased as the pressure ratio increased. The chordwise coordinate of the incremental-normal-force center of pressure remained upstream of the nozzle center line for the nozzle positions and pressure ratios of the investigation. The chordwise coordinate approached zero as the jet vertical distance beneath the wing increased. In the spanwise direction there was little change due to varying rocket-jet position and pressure ratio. Some boundary-layer flow separation on the wing was observed for the rocket jets close to the wing and at the higher pressure ratios. The magnitude of the chordwise and spanwise pressure distributions due to jet interference was greatest for rocket jets close to the wing and decreased as the jet was displaced farther from the wing.

The design procedure for the rockets used is given in the appendix.

CONFIDENTIAL

INTRODUCTION

It has been shown in reference 1 that jets exhausting laterally into supersonic streams from bodies of revolution produce some side force due to jet-interference effects. Data obtained in the Langley Pilotless Aircraft Research Division showed that rockets mounted below the wing on a free-flight model to produce a yawing disturbance also created a very large pitching disturbance and some rolling when fired. This induced lift may be used as a controlling force for high-speed missiles. The application of such a technique would simplify and lighten control systems for the missiles.

The purpose of this investigation, which is a phase of a current program to study various aspects of jet interference, was to determine the pressure loads produced on a flat-plate wing by rocket jets exhausting in the spanwise direction below the wing and perpendicular to a supersonic free stream. The variables involved were nozzle type, nozzle vertical position beneath the flat-plate wing, and the ratio of rocket-chamber pressure to free-stream static pressure. The types of nozzles used were one axially symmetric sonic nozzle (jet Mach number of 1.00), two axially symmetric supersonic nozzles (jet Mach numbers of 1.74 and 3.04), and one two-dimensional supersonic nozzle (jet Mach number of 1.71). The three vertical positions investigated were 4, 8, and 12 nozzle-throat diameters from the plate. The range of the ratio of rocket-chamber pressure to free-stream static pressure was from 0 to 130.

The tests were conducted in the 27- by 27-inch preflight jet facility of the Langley Pilotless Aircraft Research Station at Wallops Island, Va. at a free-stream Mach number of 2.0 and a free-stream Reynolds number per foot of 14.4×10^6.

SYMBOLS

C_p pressure coefficient, $p - p_\infty/q_\infty$

D   diameter

F   force, lb

M   Mach number

p   static pressure, lb/sq ft

p_t total pressure, lb/sq ft

q dynamic pressure, lb/sq ft

x/D_T ratio of chordwise distance along flat-plate wing to rocket
            nozzle-throat diameter, positive when measured from
            leading edge of vertical strut rearward

y/D_T ratio of spanwise distance across flat-plate wing to rocket
            nozzle-throat diameter, positive when measured from leading
            edge of vertical strut towards center of tunnel

$\Delta\bar{x}/D_T$ ratio of incremental chordwise distance that center of pressure
            is from rocket-nozzle center line to rocket nozzle-throat
            diameter, positive when measured downstream of center line

$\bar{y}/D_T$ ratio of spanwise location of center of pressure to nozzle-
            throat diameter, positive when measured from nozzle exit

γ ratio of specific heats of rocket exhaust gases

z/D_T ratio of vertical distance below flat-plate wing to rocket
            nozzle-throat diameter, positive when measured from lower
            surface of wing downward

ΔC_p incremental pressure coefficient, $C_{p_{on}} - C_{p_{off}}$

ΔF_N incremental normal force, $\left(\iint \Delta C_p \, dx \, dy\right) q_\infty$

Subscripts:

c   rocket chamber

j   jet-exit station

N   normal

T   nozzle-throat station

∞ free stream

on   rocket operating

off   rocket not operating

APPARATUS

Preflight Jet Facility

The tests were conducted in the preflight-jet facility of the Langley Pilotless Aircraft Research Station at Wallops Island, Va. A description of this facility is given in reference 2. A Mach number 2.0, 27-inch-square nozzle was used for all tests. A photograph of the test setup is shown as figure 1.

Wing

A steel flat plate, 1/2 inch thick, was used to simulate a two-dimensional wing and this plate was made to span the exit (27-inch) nozzle. The wing was welded to supports that were bolted to the exit flange of the preflight-jet nozzle. The leading edge of the wing had an 8° bevel on the upper surface and protruded approximately 3 inches upstream into the preflight-jet nozzle exit. The wing had a rectangular plan form and a chord of $16\frac{3}{8}$ inches. Static-pressure orifices were installed on the wing lower surface and their positions are shown in figure 2.

Vertical Strut

The vertical plate which was bolted to the wing was fabricated from 1/2-inch-thick steel plate. The leading edge was beveled to 18° and was located 1.5 inches upstream of the exit plane of the preflight-jet nozzle exit. The strut was located 3 inches from the side wall of the jet. This was done to keep the strut free of the boundary-layer buildup present along the tunnel nozzle wall. The strut had a chord of 15 inches and included provisions for mounting rocket motors in three positions: A, B, and C. These positions were located at x/D_T of 24, 17.5, and 10.5 downstream of the strut and z/D_T of 4, 8, and 12 beneath the flat-plate wing. The rocket-nozzle exits were faired with the inner surface of the vertical strut, and located downstream of these nozzle exits were a total of nine static-pressure orifices. Figure 2 illustrates the arrangement of the flat-plate wing, vertical strut, and rocket-nozzle locations. This figure also shows the locations of the strut orifices.

Rockets

Figure 3 is a detailed drawing of the rocket nozzles used in the investigation. The throat areas were the same for all the rocket

nozzles; thus, the two-dimensional nozzle has an equivalent throat diameter equal to the throat diameter of the axisymmetric nozzles. The rectangular exit of the two-dimensional nozzle was oriented such that the long side of the rectangular section was vertical. All distances from nozzle exits are expressed in terms of nozzle-throat diameters or equivalent throat diameter.

Specially designed solid-propellant rockets generated the hot exhaust gases ($\gamma = 1.25$). These rockets were designed to give a triangular chamber-pressure impulse and to operate within a range of 0 to 1,800 pounds per square inch in a time interval of 0.8 second. (See fig. 4.) The range of chamber pressure varied some from rocket to rocket because of variations in burning characteristics of the solid propellants and, also, because of different amounts of nozzle losses. A detailed description of the design, performance, and components of the rockets is given in the appendix.

INSTRUMENTATION

The pressures at the head end of the rocket chamber were measured for all tests. The pressure distributions on the flat-plate wing were measured by Statham pressure gages and by two 6-cell pressure units. These gages and cells were connected to 0.06-inch-diameter wing orifices by 1/8-inch copper tubing. The chordwise and spanwise locations of these wing static-pressure orifices are shown in figure 2.

Nine static-pressure orifices 0.06 inch in diameter supplied some static-pressure data on the inner surface of the vertical strut. The locations for these orifices are also shown in figure 2. The free-stream total and static pressures of the preflight-jet nozzle exit were measured for all tests so that free-stream dynamic pressure and pressure coefficients could be computed. Four oscillograph recorders and two 6-cell pressure recorders were used to register all the data obtained for this investigation.

ACCURACY

The accuracy of the measurements, based on instrument accuracy and errors in reading and plotting the data, was estimated to vary within the following limits:

M_∞ . . . . ± 0.020

$P_{t,c}/P_\infty$ . . . . ± 0.500

ΔC_p . . . . ± 0.013

F_j . . . . ± 0.500

One test was repeated and the results obtained agreed favorably with a comparable one and were within the tolerances just presented.

Any transient effects which may have been inherent in the system appeared to be negligible, since an examination of plots of ΔC_p as a function of increasing and decreasing pressure ratio revealed no appreciable discrepancies.

The alinement of the flat-plate wing, vertical strut, and rocket-nozzle center lines is believed to be within $\pm 1^\circ$.

TEST PROCEDURE

The main measurements made during each test were: wing static pressures, strut static pressures, preflight-jet total and static pressures, and rocket-chamber pressures.

Static tests of four rockets were made in the Langley Pilotless Aircraft Research Division rocket test area. Each rocket tested used one of the four nozzle types incorporated in this investigation. The rocket thrust and chamber pressure were measured during each static test, and from these measurements calibration curves of jet static pressure as a function of rocket-chamber pressure for each nozzle type were obtained. A description of how these calibration curves were obtained is included in the appendix. Each nozzle type was tested in the three positions (A, B, and C) beneath the flat-plate wing, and pressure-distribution data on wing and strut were obtained. Complete pressure-distribution data on the flat-plate wing for the sonic ($M_j = 1.00$) and supersonic ($M_j = 1.74$) nozzles in positions A, B, and C have been presented; whereas, only data on the wing for the rockets with supersonic nozzle ($M_j = 3.04$) in positions A and C and with two-dimensional supersonic nozzle ($M_j = 1.71$) in positions A and B have been presented herein. Because of rocket misfires the data for positions B and C were not obtained for the supersonic and two-dimensional supersonic nozzles, respectively.

All the pressure measurements taken on the wing and strut were within the Mach diamond of the preflight-jet nozzle.

METHOD OF ANALYSIS

The interference pressures due to the presence of the jet were obtained by subtracting the jet-off pressure measurements from the jet-on pressure measurements. Although the wing was a flat plate, warpage in the plate resulted in small pressure coefficients at zero lift.

The incremental normal force on the flat-plate wing was obtained by integrating graphically the incremental pressure coefficients over the wing surface.

The center of pressure for the incremental pressure loads for the sonic nozzle in positions A, B, and C and for several pressure ratios was obtained graphically by integrating the chordwise and spanwise moments over the wing. The total moments were then divided by the incremental normal force to obtain chordwise and spanwise coordinates of the center of pressure. Since the chordwise coordinates for the positions A, B, and C also varied, the center-of-pressure results are presented in terms of $\Delta\bar{x}$. These coordinates have been referenced to the nozzle-throat diameter.

The presence of flow separation was determined by the criterion of double peak in the chordwise pressure distribution as in references 3 and 4. The roughness Reynolds number was 4,625 calculated for the first spanwise row of wing orifices, and according to reference 5 this value was well above the transition Reynolds number. Hence, the analysis that follows assumes a turbulent boundary layer along the wing.

FLOW PHENOMENA

A brief description of the flow field existing about a jet issuing perpendicular to an external supersonic stream and the nomenclature used herein may be helpful in discussing the plots that follow. Figure 5 illustrates diagrammatically a chordwise section of the flow field existing around such a jet with the parts of the jet and flow field labeled. When the jet-exit static pressure is greater than the external-flow static pressure, the jet will expand as it leaves the nozzle. This expanding jet is initially perpendicular to the external flow and immediately upon leaving the nozzle exit begins to turn in the direction of the supersonic flow. A primary shock wave forms in the region just upstream of the issuing jet boundary. In the plan-form view the primary shock wave varies from normal (maximum shock strength) just upstream of

the jet exit to oblique in the spanwise direction. This shock pattern exhibits the same characteristics in the vertical plane. The region between the primary shock wave and jet boundary will experience positive pressures and the magnitude of these positive pressures will diminish as the primary shock-wave angle decreases with respect to the stream direction. The pressure reaches a positive peak at the primary shock and then an expansion of the flow causes negative pressures. Then, a recompression brings the negative values to slightly below free-stream conditions. This recompression may be due to a wake shock (considering the jet as a solid body), a jet shock originating within the jet, or a combination of both. Schileren photographs of some actual flow fields existing about side jets exhausting into supersonic main streams are shown in reference 1.

RESULTS AND DISCUSSION

Wing pressure data are presented in tables 1 to 10 as incremental pressure coefficients for the following variables: nozzle geometry, nozzle position, and pressure ratio. The effects of these variables on wing pressure distributions (as a result of shock location and boundary-layer separation), loads, and centers of pressure are discussed in the following sections. Because of insufficient pressure data on the strut, no discussion of the incremental vertical-strut pressures is made; only the tabulated data (tables 11 to 14) are presented.

Incremental Wing Pressures

Since the rocket-chamber pressures varied during each test, values of ΔC_p for $p_{t,c}/p_\infty$ in increments of 10 have been given in tables 1 to 10. The variations of chordwise and spanwise ΔC_p are presented for a value of $p_{t,c}/p_\infty$ of 58 in figures 6 to 9 and for a value of $p_{t,c}/p_\infty$ of 120 in figure 10. In general, these plots show the same characteristics: namely, in the chordwise direction the pressure rises to maximum values, then a rapid expansion of the flow causes negative coefficients, and a recompression brings the negative values to near free-stream conditions. In the spanwise direction ΔC_p diminishes in magnitude from a maximum near the nozzle exit to near free-stream conditions at distances greater than 30 nozzle throat diameters from the exit.

These plots also indicate that the effects on pressure distributions due to nozzle geometries were small; whereas, the effects on induced wing pressures due to nozzle position and pressure ratio appear to be more pronounced. The induced pressures were the greatest when the rocket jets were located at position A and were the least at position C. As the pressure ratio was increased, the magnitude of the

induced wing pressures also increased. These results were due mainly to the angle the primary shock makes with the wing at the intersection point. For the rocket jets close to the wing (position A), the angle was the greatest and, hence, the magnitude of the induced pressures was the greatest. Increasing the pressure ratio increased the shock angle and thus caused even greater induced pressures on the wing. (See figs. 7 and 10 for a comparison of pressure distributions for nozzle position A at values of $p_{t,c}/p_\infty$ of 58 and 120.)

The fact that the more intense portion of the primary shock intersected the wing for positions A and B rather than for position C for all nozzle types caused the boundary-layer flow to separate in some regions forward of the primary shock for positions A and B. This is evident from the initial shape of the chordwise pressure-distribution curves, as reported in references 3 and 4 for turbulent separated flow, since the initial portions of the pressure-distribution curves have a double peak. The chordwise pressure variations (up to the maximum peak point) obtained at y/D_T of 2.5 for the sonic nozzle in positions A and B were similar to that observed about a forward-facing step with separated boundary layer in reference 3. An incremental pressure coefficient of approximately 0.35 measured for the first pressure peaks from distributions for positions A and B agreed favorably with the turbulent-boundary-layer value (0.335) measured on a flat plate from the step technique of reference 3 at a free-stream Mach number of 2.0.

Integrated Loads

The incremental force obtained was divided by the rocket thrust and this force ratio is plotted as a function of pressure ratio in figure 11. The force ratio varied approximately between 1 and 2 and generally decreased with increasing pressure ratio. Figure 11(a) shows that, generally, at any pressure ratio the force ratio decreases as the sonic nozzle is moved away from the wing. This is the same result that was obtained in reference 6 for jets exhausting downstream. Figure 11(b) shows that the two-dimensional supersonic nozzle ($M_j = 1.71$) induced loads that were about half as large as those induced by the $M_j = 1.0$ and 1.74 nozzles; whereas, the $M_j = 3.04$ nozzle induced loads that were about 70 percent as large.

Center of Pressure

The variation of incremental normal-force center of pressure for chordwise and spanwise directions is illustrated in figure 12 for only one case, that of the sonic nozzle operating at $p_{t,c}/p_\infty$ of 50, 75, and 100.

Figure 12(a) shows that the spanwise location of center of pressure varies little as the vertical distance of the jet from the wing is varied. In general, the $\bar{y}/D_T$ moves closer to the nozzle exit as $p_{t,c}/p_\infty$ is increased to 100. The decrease of $\bar{y}/D_T$ as total pressure ratio is increased appears plausible, since at the higher pressure ratios the jet expands more and has more resistance to bending. This causes a more intense portion of the primary shock wave to intersect the wing in the region near the nozzle exits.

Figure 12(b) shows the effect on chordwise location of the center of pressure as vertical distance and pressure ratio are varied. The chordwise location $\Delta\bar{x}/D_T$ remains forward of the nozzle center line for the range of vertical distance and total pressure ratio covered. The chordwise location $\Delta\bar{x}/D_T$ moves toward the nozzle center line with increase in nozzle vertical distance from the wing and it moved upstream as $p_{t,c}/p_\infty$ was increased. The chordwise location came closest to the nozzle center line ($\Delta\bar{x}/D_T = -1.17$) for a value of z/D_T of 12 and $p_{t,c}/p$ of 50.

SUMMARY OF RESULTS

An experimental investigation was conducted to determine the pressure loads produced on a flat-plate wing by rocket jets exhausting in a spanwise direction beneath the wing and perpendicular to a supersonic free stream. The tunnel free-stream Mach number at the test section was 2.0 and the free-stream Reynolds number per foot was 14.4×10^6. The results of varying the nozzle type, nozzle position, and pressure ratio may be summarized as follows:

1. The incremental normal force due to jet interference on the wing varied from one to two times the rocket thrust and generally decreased as the pressure ratio increased.

2. Although the magnitude of the incremental pressures decreased as the jet was displaced farther away from the wing, the incremental normal force decreased only slightly.

3. The supersonic nozzle (jet Mach number M_j of 3.04) induced loads that were about 70 percent as large as those induced by the sonic nozzle ($M_j = 1.00$) and the supersonic nozzle ($M_j = 1.74$); whereas, the two-dimensional supersonic nozzle ($M_j = 1.71$) induced loads that were about half as large.

4. The spanwise ordinate of the interference center of pressure indicated small movement as the nozzle position was varied.

5. The chordwise ordinate of the center of pressure remained upstream of the rocket-nozzle center line for the range of vertical position and pressure ratios covered. As the vertical distance of the jet was increased, the center of pressure moved closer to the rocket-nozzle center line and as the pressure ratio was increased, the center of pressure moved farther upstream from the rocket-nozzle center line.

6. Boundary-layer separation was observed for the jets in the close positions to the wing and for higher pressure ratios.

Langley Aeronautical Laboratory,
 National Advisory Committee for Aeronautics,
  Langley Field, Va., March 21, 1958.

APPENDIX

DESIGN PROCEDURE FOR ROCKETS EMPLOYED

In order to illustrate the design procedure, the actual rocket parameters which were required for this investigation are used herein and are presented as follows:

Range of $p_{t,c}/p_\infty$ from 0 to 130
Relative symmetric time-history variation of $p_{t,c}/p_\infty$
Rocket operating time of 0.6 to 0.8 second
Back pressure p_∞ of 14.7 pounds per square inch absolute

Internal Ballistics Relationships

For the rocket operating at equilibrium conditions, the mass rate of gases generated by combustion of the solid propellant must be equal to the mass rate of gases discharged through the rocket nozzle - namely,

$$m_g = m_d \tag{1}$$

The mass rate of gases generated is a function of the solid-propellant density, the exposed propellant area, and the linear burning rate of the propellant, which can be written as

$$m_g = \rho S b \tag{2}$$

where the linear burning rate is defined as

$$b = C p_{t,c}^n \tag{3}$$

Substituting equation (3) into equation (2) gives

$$m_g = \rho S C p_{t,c}^n \quad , \tag{4}$$

where

C   coefficient in equation (3) which is a function of propellant

$p_{t,c}$ rocket-chamber total pressure, lb/sq in.

n   function of propellant

ρ density of solid propellant, lb/cu in.

S   exposed solid-propellant area to combustion flame, sq in.

From equation (1), the mass rate of gases discharged can be written as a function of a discharge coefficient, rocket nozzle-throat area, and rocket-chamber total pressure:

$$m_d = C_D A_t p_{t,c} \qquad\qquad (5)$$

where C_D, the discharge coefficient, is defined as the mass rate of flow possible when a given powder composition is burned in a rocket motor having a unit throat area and a unit chamber pressure. The discharge coefficient C_D remains relatively constant throughout the combustion process. Thus, the burning surface of the solid propellant must vary according to the following equations:
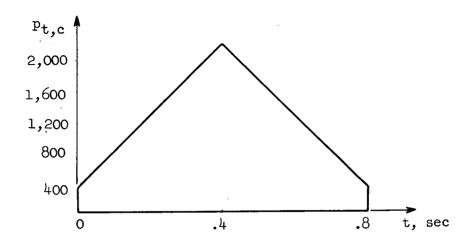
$$S = \frac{C_D A_t p_{t,c}}{\rho b} \qquad\qquad (6a)$$

or

$$S = \frac{C_D A_t}{\rho C}\left(p_{t,c}\right)^{1-n} \qquad\qquad (6b)$$

Propellant Design

In order to cover the desired pressure-ratio range for this investigation, the combustion-chamber pressure was varied as shown in the following diagram:

$p_{t,c}$

2,000

1,600

1,200

800

400

0   .4   .8   t, sec

The other important parameters necessary in designing the propellant have been fixed at the following values:

c_D = 0.0073

A_t = 0.0314 sq in.

ρ = 0.057 lb/cu in.
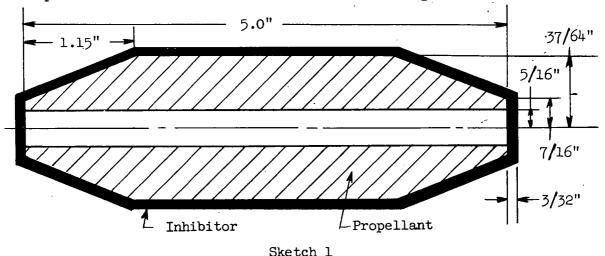
p_∞ = 14.7 lb/sq in. abs

b   (See fig. 13 for these values), in./sec

A Cordite SU/K solid-propellant rocket grain was chosen as the propellant and was modified to meet the requirements. The Cordite grain is easily machined and its burning-rate curve (fig. 13) fitted the requirements. The initial length and maximum diameter of the grain were fixed by the size of the rocket. By using equations (6) with the given data, a time history of the exposed burning area was obtained. From these data the thickness and external shape of the grain were easily arrived at. The resulting shape of the grain used was a right circular cylinder with an initial hole through the center whose diameter was dictated by the initial exposed burning area. On

the external surface the grain had tapered end sections which were
dictated by the requirement that the time history of the pressure ratio
be symmetrical about its peak value. Thus, the condition that it burn
radially - from center outward - was imposed on the grain. The control
of the exposed burning area was achieved by bonding an inhibitor
(nonburning material) to all external surfaces of the grain. The grain
shape and its dimensions are shown in the following sketch:

Sketch 1

Rocket Components

A photograph of the rocket components used in the investigation is
presented as figure 14. The rocket components consisted of a nozzle,
director tube and grid, igniter holder, chamber-pressure tube, and pres-
sure fittings for sealing off igniter holder. The nozzles were made
interchangeable with the rocket cases, so that any one of the four nozzle
types tested could be used with any of the rocket cases. All the parts
were made from low-carbon steel except the rocket cases, which were made
from AISI 4130 steel, and the pressure fittings, which were made of
brass. The rocket cases were heat-treated to withstand pressures up to
100,000 pounds per square inch.

Tests

Four grains were machined according to the dimensions shown in
sketch 1 and the external surfaces including the ends were coated with
an inhibitor composed of cellulose acetate and epoxy resin cement.
These grains were fitted to rocket cases and were statically tested to
obtain the rocket performance for each nozzle type used in the investi-
gation. The rocket-chamber pressure agreed favorably with the design

values, and for comparison the actual results for two of the firings have been superposed upon the design curve which is shown in figure 15.

Calibration Curves

The rocket thrust and chamber pressure were measured during each static firing, and calibration curves of rocket-chamber pressure as a function of jet-exit static pressure for each nozzle type has been obtained. These curves are shown in figure 16. The jet-exit static pressure was obtained from the thrust equation:

$$F_j = p_j A_j \left(\gamma M_j{}^2 + 1\right) - p_\infty A_j \tag{7}$$

by solving for p_j

$$p_j = \frac{F_j + p_\infty A_j}{A_j \left(\gamma M_j{}^2 + 1\right)} \tag{8}$$

where

A_j jet-exit area, sq in.

γ ratio of specific heats for the propellant $(\gamma = 1.25)$

M_j Mach number at jet exit

p_∞ free-stream static pressure, lb/sq in. abs

p_j jet-exit static pressure, lb/sq in. abs

Since the rocket-chamber pressures were measured during each tunnel run, the thrust of the rockets was obtained by choosing values of p_j from the calibration curves and computing by use of equation (7) the thrust for the existing back pressure.

REFERENCES

1. Morkovin, M. U., Pierce, C. A., Jr., and Craven, C. E.: Interaction of a Side Jet With a Supersonic Main Stream. Bull. No. 35, Eng. Res. Inst., Univ. of Michigan, Sept. 1952.

2. Faget, Maxime A., Watson, Raymond S., and Bartlett, Walter A., Jr.: Free-Jet Tests of a 6.5-Inch-Diameter Ram-Jet Engine at Mach Numbers of 1.81 and 2.00. NACA RM L50L06, 1951.

3. Lange, Roy H.: Present Status of Information Relative to the Prediction of Shock-Induced Boundary-Layer Separation. NACA TN 3065, 1954.

4. Chapman, Dean R., Kuehn, Donald M., and Larson, Howard K.: Preliminary Report on a Study of Separated Flows in Supersonic and Subsonic Streams. NACA RM A55L14, 1956.

5. Braslow, Albert L.: Effect of Distributed Granular-Type Roughness on Boundary-Layer Transition at Supersonic Speeds With and Without Surface Cooling. NACA RM L58A17, 1958.

6. Leiss, Abraham, and Bressette, Walter E.: Pressure Distribution Induced on a Flat Plate by a Supersonic and Sonic Jet Exhaust at a Free-Stream Mach Number of 1.80. NACA RM L56I06, 1957.

TABLE 1.- WING PRESSURES FOR SONIC NOZZLE AT POSITION A

Orifice ordinates		Incremental wing pressure coefficients for $p_{t,c}/p_\infty$ of -											
x/D_T	y/D_T	10	20	30	40	50	60	70	80	90	100	110	120	130
11.5	2.5					0	0	0	0	0	0	0		
14.0	2.5					0	0	0	0	.005	.033	.035		
19.0	2.5					.165	.220	.267	.305	.335	.348	.350		
21.5	2.5					.307	.347	.379	.400	.405	.420	.437		
24.0	2.5					.500	.580	.635	.770	.805	.900	.875		
26.5	2.5					.410	.300	.200	.138	.092	.079	.075		
29.0	2.5					-.082	-.120	-.147	-.155	-.155	-.153	-.150		
34.0	2.5					-.250	-.250	-.255	-.265	-.275	-.280	-.283		
39.0	2.5					-.042	-.045	-.050	-.058	-.068	-.092	-.112		
44.0	2.5					-.023	-.024	-.025	-.030	-.036	-.045	-.056		
49.0	2.5					-----								
54.0	2.5					-.025	-.023	-.022	-.023	-.026	-.030	-.035		
64.0	2.5					-.015	-.015	-.012	-.015	-.015	-.018	-.020		
11.5	7.5					0	0	0	0	0	0	0		
14.0	7.5					0	0	0	0	0	.001	.010		
19.0	7.5					.075	.130	.185	.230	.257	.275	.285		
21.5	7.5					.200	.225	.247	.269	.285	.290	.269		
24.0	7.5					.235	.247	.250	.230	.250	.285	.329		
26.5	7.5					.240	.262	.325	.420	.515		.725		
31.5	7.5					.100	.100	.087	.070	.060	.050	.041		
36.5	7.5					-.080	-.112	-.130	-.141	-.150	-.155	-.160		
41.5	7.5					-.120	-.140	-.159	-.162	-.165	-.167	-.169		
46.5	7.5					-.015	-.020	-.023	-.031	-.038	-.046	-.057		
51.5	7.5					-.025	-.027	-.030	-.034	-.028	-.034	-.036		
61.5	7.5					-.025	-.027	-.027	-.031	-.028	-.028	-.028		
9.0	12.5					0	0	0	0	0	0	0		
16.5	12.5					-----	-----	-----	-----	-----	-----	-----		
19.0	12.5					.010	.011	.060	.122	.165	.190	.195		
21.5	12.5					-----	-----	-----	-----	-----	-----	-----		
24.0	12.5					.150	.168	.187	.194	.197	.190	.174		
26.5	12.5					.157	.165	.161	.142	.120	.110	.107		
29.0	12.5					.130	.125	.119	.114	.114	.124	.137		
34.0	12.5					.089	.095	.106	.125	.135	.140	.142		
39.0	12.5					0	0	0	-.001	-.008	-.016	-.028		
49.0	12.5					-.060	-.080	-.097	-.110	-.115	-.120	-.125		
59.0	12.5					-.020	-.020	-.021	-.022	-.025	-.026	-.030		
19.0	17.5					0	0	0	.013	.062	.125	.172		
24.0	17.5					.013	.080	.122	.143	.153	.155	.152		
26.5	17.5					.092	.122	.136	.142	.140	.139	.136		
31.5	17.5					.092	.110	.107	.095	.073	.053	.035		
36.5	17.5					.075	.063	.053	.050	.050	.053	.058		
41.5	17.5					.018	.018	.018	.020	.025	.030	.035		
61.5	17.5					-.016	-.020	-.022	-.025	-.029	-.033	-.037		
31.5	25.0													
39.0	25.0					.070	.072	.075	.073	.066	.057	.046		
54.0	25.0					.005	.005	.005	.005	0	-.012	-.015		
59.0	25.0					-.015	-.018	-.020	-.023	-.025	-.027	-.030		
64.0	25.0													
41.5	30.0													
46.5	30.0					.048	.050	.065	.068	.058	.042	.038		
51.5	30.0													
61.5	30.0					-.005	-.005	-.005	-.005	-.005	-.006	-.007		

TABLE 2.- WING PRESSURES FOR SONIC NOZZLE AT POSITION B

Orifice ordinates		Incremental wing pressure coefficients for $p_{t,c}/p_\infty$ of -											
x/D_T	y/D_T	10	20	30	40	50	60	70	80	90	100	110	120	130
11.5	2.5			0.001	0.004	0.006	0.006	0.009	0.016	0.030	0.054			
14.0	2.5			0	0	0	.035	.062	.082	.091	.091			
19.0	2.5			.210	.276	.422	.428	.375	.365	.373	.390			
21.5	2.5			.250	.296	.301	.312	.322	.330	.332	.340			
24.0	2.5			.148	.170	.168	.168	.168	.167	.167	.168			
26.5	2.5			.037	.045	.045	.044	.038	.035	.030	.028			
29.0	2.5			-.041	-.049	-.056	-.061	-.064	-.068	-.072	-.077			
34.0	2.5			-.066	-.096	-.115	-.127	-.136	-.142	-.146	-.147			
39.0	2.5			-.016	-.030	-.040	-.045	-.060	-.070	-.074	-.075			
44.0	2.5			-.011	-.017	-.019	-.016	-.016	-.021	-.035	-.037			
49.0	2.5			-----	-----	-----	-----	-----	-----	-----	-----			
54.0	2.5			-.009	-.010	-.013	-.014	-.015	-.015	-.016	-.016			
64.0	2.5			-.005	-.007	-.011	-.013	-.014	-.014	-.015	-.015			
11.5	7.5			0	0	0	0	0	0	0	0			
14.0	7.5			0	0	0	0	.020	.055	.091	.143			
19.0	7.5			.102	.175	.229	.268	.301	.331	.356	.374			
21.5	7.5			.198	.248	.271	.283	.300	.318	.335	.353			
24.0	7.5			.185	.195	.205	.212	.227	.240	.246	.254			
26.5	7.5			.042	.045	.045	.046	.047	.048	.047	.045			
31.5	7.5			-.030	-.038	-.045	-.050	-.057	-.062	-.070	-.075			
36.5	7.5			-.050	-.070	-.092	-.100	-.104	-.108	-.115	-.117			
41.5	7.5			-.025	-.042	-.065	-.075	-.090	-.100	-.111	-.115			
46.5	7.5			-.015	-.016	-.014	-.012	-.015	-.017	-.022	-.029			
51.5	7.5			-.006	-.008	-.009	-.011	-.012	-.012	-.012	-.012			
61.5	7.5			-.007	-.010	-.011	-.012	-.013	-.014	-.015	-.016			
9.0	12.5			0	0	0	0	0	0	0	0			
16.5	12.5			0	0	0	0	.010	.045	.094	.141			
19.0	12.5			0	0	.037	.095	.160	.196	.220	.235			
21.5	12.5			.035	.108	.169	.200	.230	.250	.266	.275			
24.0	12.5			.137	.192	.217	.232	.247	.258	.272	.281			
26.5	12.5			.154	.179	.185	.194	.195	.200	.204	.209			
29.0	12.5			.100	.115	.115	.115	.111	.111	.110	.110			
34.0	12.5			0	0	-.011	-.017	-.023	-.028	-.031	-.036			
39.0	12.5			-.050	-.057	-.065	-.072	-.079	-.083	-.089	-.095			
49.0	12.5			-.018	-.025	-.031	-.040	-.050	-.062	-.075	-.085			
59.0	12.5			-.007	-.009	-.010	-.011	-.010	-.012	-.010	-.007			
19.0	17.5			0	0	0	0	.021	.050	.081	.085			
24.0	17.5			.005	.039	.088	.117	.138	.150	.157	.165			
26.5	17.5			.055	.113	.145	.158	.165	.177	.183	.190			
31.5	17.5			.110	.122	.125	.126	.128	.132	.133	.135			
36.5	17.5			.056	.059	.052	.050	.046	.042	.040	.040			
41.5	17.5			-.012	-.019	-.024	-.029	-.031	-.036	-.037	-.036			
61.5	17.5			-.006	-.009	-.010	-.010	-.010	-.010	-.010	-.010			
31.5	25.0													
39.0	25.0			.083	.090	.090	.090	.090	.090	.092	.095			
54.0	25.0			-.015	-.018	-.020	-.022	-.023	-.025	-.026	-.027			
59.0	25.0			-.036	-.043	-.045	-.049	-.050	-.050	-.051	-.052			
64.0	25.0													
41.5	30.0													
46.5	30.0			.065	.065	.065	.065	.066	.067	.067	.065			
51.5	30.0													
61.5	30.0			-.015	-.016	-.017	-.018	.019	-.020	-.020	-.020			

TABLE 3.- WING PRESSURES FOR SONIC NOZZLE AT POSITION C

Orifice ordinates		Incremental wing pressure coefficients for $p_{t,c}/p_\infty$ of -												
x/D_T	y/D_T	10	20	30	40	50	60	70	80	90	100	110	120	130
11.5	2.5	0	0	0	0	0	0.005	0.023	0.062	0.115	0.170			
14.0	2.5	.005	.010	.016	.022	.058	.133	.211	.275	.327	.358			
19.0	2.5	.056	.128	.203	.243	.275	.287	.297	.295	.292	.275			
21.5	2.5	.103	.148	.171	.180	.180	.180	.175	.170	.162	.150			
24.0	2.5	.078	.092	.095	.095	.095	.094	.091	.087	.086	.084			
26.5	2.5	.031	.033	.031	.030	.029	.027	.025	.023	.021	.018			
29.0	2.5	-.005	-.010	-.020	-.021	-.021	-.025	-.026	-.030	-.030	-.032			
34.0	2.5	-.037	-.055	-.077	-.087	-.095	-.100	-.105	-.108	-.110	-.112			
39.0	2.5	-.020	-.028	-.033	-.033	-.031	-.032	-.033	-.037	-.060	-.095			
44.0	2.5	-.011	-.017	-.021	-.024	-.025	-.032	-.045	-.050	-.046	-.043			
49.0	2.5	-.010	-.013	-.014	-.015	-.016	-.020	-.022	-.025	-.022	-.020			
54.0	2.5	0	0	-.005	-.005	-.005	-.007	-.007	-.010	-.010	-.012			
64.0	2.5	0	0	0	0	0	0	0	0	0	0			
11.5	7.5	0	.003	.005	.005	.005	.005	.005	.006	.019	.036			
14.0	7.5	0	0	.002	.005	.005	.027	.110	.187	.242	.272			
19.0	7.5	.038	.110	.184	.238	.268	.285	.295	.305	.311	.315			
21.5	7.5	.069	.162	.193	.205	.210	.215	.217	.217	.218	.220			
24.0	7.5	.110	.132	.130	.128	.128	.125	.124	.123	.122	.122			
26.5	7.5	.020	.025	.026	.025	.024	.022	.020	.019	.016	.016			
31.5	7.5	-.025	-.030	-.035	-.036	-.038	-.044	-.046	-.053	-.058	-.064			
36.5	7.5	-.040	-.060	-.070	-.080	-.087	-.092	-.096	-.100	-.103	-.102			
41.5	7.5	-.016	-.021	-.021	-.023	-.026	-.030	-.043	-.070	-.090	-.100			
46.5	7.5	-.015	-.024	-.028	-.028	-.025	-.027	-.040	-.045	-.045	-.035			
51.5	7.5	-.010	-.014	-.012	-.009	-.011	-.012	-.015	-.014	-.013	-.012			
61.5	7.5	0	0	0	0	0	0	0	0	0	0			
9.0	12.5	0	0	0	0	0	0	0	0	0	0			
16.5	12.5	0	0	0	0	0	.022	.090	.143	.173	.183			
19.0	12.5	.005	.013	.035	.075	.127	.180	.220	.248	.266	.283			
21.5	12.5	.027	.081	.143	.186	.215	.236	.253	.266	.278	.288			
24.0	12.5	.056	.141	.178	.191	.193	.191	.195	.197	.199	.200			
26.5	12.5	.092	.130	.131	.130	.128	.125	.124	.122	.120	.118			
29.0	12.5	.078	.072	.065	.063	.061	.058	.055	.052	.049	.046			
34.0	12.5	-.003	-.015	-.020	-.023	-.024	-.030	-.034	.038	-.042	-.045			
39.0	12.5	-.050	-.057	-.060	-.065	-.067	-.070	-.073	-.076	-.080	-.083			
49.0	12.5	0	-.005	-.010	-.015	-.021	-.022	-.024	-.031	-.045	-.062			
59.0	12.5	-.005	-.005	-.006	-.007	-.008	-.010	-.011	-.012	-.015	-.017			
19.0	17.5	.003	.005	.007	.008	.010	.031	.073	.102	.120	.131			
24.0	17.5	.003	.023	.062	.095	.122	.140	.156	.173	.190	.206			
26.5	17.5	.020	.073	.118	.142	.150	.159	.166	.175	.183	.191			
31.5	17.5	.072	.102	.104	.105	.104	.102	.099	.094	.089	.087			
36.5	17.5	.038	.030	.025	.023	.021	.017	.013	.010	.005	0			
41.5	17.5	-.020	-.030	-.032	-.032	-.033	-.035	-.040	-.045	-.047	-.055			
61.5	17.5	0	0	-.002	-.004	-.005	-.006	-.007	-.008	-.009	-.011			
31.5	25.0	.016	.035	.051	.063	.073	.080	.085	.088	.090	.090			
39.0	25.0	.041	.074	.075	.075	.074	.072	.070	.070	.070	.070			
54.0	25.0	-.022	-.030	-.027	-.025	-.026	-.033	-.038	-.040	-.041	-.041			
59.0	25.0	-.010	-.015	-.015	-.018	-.027	-.042	-.047	-.047	-.046	-.046			
64.0	25.0	-.010	-.017	-.020	-.024	-.027	-.031	-.035	-.035	-.035	-.036			
41.5	30.0	.031	.050	.061	.066	.070	.070	.068	.067	.065	.063			
46.5	30.0	.035	.052	.054	.055	.052	.050	.047	.047	.046	.045			
51.5	30.0	-.008	-.010	-.012	-.015	-.015	-.015	-.015	-.015	-.013	-.013			
61.5	30.0	-.015	-.023	-.027	-.030	-.031	-.032	-.032	-.032	-.032	-.031			

TABLE 4.- WING PRESSURES FOR SUPERSONIC NOZZLE (M_j = 1.74) AT POSITION A

Orifice ordinates		Incremental wing pressure coefficients for $P_{t,c}/P_\infty$ of -												
x/D_T	y/D_T	10	20	30	40	50	60	70	80	90	100	110	120	130
11.5	2.5			0.007	0.007	0.008	0.010	0.010	0.010	0.011	0.013	0.015	0.015	0.015
14.0	2.5			0	0	0	0	0	0	.002	.012	.025	.049	.088
19.0	2.5			0	.025	.051	.082	.125	.189	.262	.310	.339	.362	.378
21.5	2.5			.105	.134	.340	.490	.525	.514	.480	.454	.440	.442	.448
24.0	2.5			.580	.585	.541	.532	.528	.525	.525	.523	.519	.518	.514
26.5	2.5			.270	.306	.280	.244	.211	.190	.176	.168	.163	.160	.159
29.0	2.5			-.041	-.053	-.085	-.110	-.127	-.140	-.150	-.158	-.163	-.168	-.170
34.0	2.5			-.120	-.170	-.188	-.190	-.204	-.198	-.190	-.187	-.186	-.184	-.192
39.0	2.5			-.045	-.053	-.060	-.068	-.086	-.105	-.120	-.135	-.147	-.155	-.155
44.0	2.5			-.030	-.034	-.040	-.043	-.047	-.051	-.056	-.062	-.068	-.075	-.085
49.0	2.5			-.008	-.008	-.027	-.040	-.045	-.045	-.045	-.048	-.050	-.052	-.052
54.0	2.5			-.012	-.014	-.015	-.017	-.020	-.023	-.025	-.025	-.027	-.029	-.030
64.0	2.5			-.005	-.007	-.009	-.010	-.012	-.013	-.015	-.015	-.017	-.018	-.019
11.5	7.5			.005	.005	.005	.005	.005	.005	.006	.008	.009	.010	.010
14.0	7.5			.008	.008	.008	.008	.008	.010	.010	.015	.025	.040	.065
19.0	7.5			.012	.020	.070	.134	.195	.236	.268	.295	.317	.337	.356
21.5	7.5			.095	.178	.234	.273	.307	.334	.354	.367	.375	.377	.375
24.0	7.5			.233	.276	.310	.339	.366	.393	.434	.504	.596	.671	.675
26.5	7.5			.084	.090	.104	.125	.161	.215	.264	.250	.195	.168	.138
31.5	7.5			.035	.050	.074	.100	.107	.074	.069	-.005	-.048	-.080	-.100
36.5	7.5			-.055	-.065	-.068	-.077	-.088	-.105	-.115	-.130	-.143	-.148	-.150
41.5	7.5			-.060	-.083	-.100	-.116	-.124	-.125	-.100	-.073	-.065	-.068	-.078
46.5	7.5			-.018	-.016	-.020	-.028	-.048	-.077	-.097	-.106	-.110	-.106	-.100
51.5	7.5			-.025	-.025	-.025	-.021	-.022	-.025	-.027	-.031	-.035	-.036	-.044
61.5	7.5			-.016	-.017	-.018	-.020	-.020	-.023	-.025	-.025	-.026	-.027	-.030
9.0	12.5			0	0	0	0	0	0	0	0	0	0	0
16.5	12.5			0	0	0	0	0	0	0	.011	.027	.037	.110
19.0	12.5			0	0	0	0	.015	.055	.107	.165	.210	.242	.268
21.5	12.5			.005	.005	.047	.115	.170	.210	.242	.269	.295	.320	.339
24.0	12.5			.070	.110	.177	.213	.231	.254	.280	.296	.300	.283	.250
26.5	12.5			.140	.164	.194	.210	.220	.220	.219	.211	.201	.203	.210
29.0	12.5			.147	.157	.170	.180	.185	.180	.177	.175	.174	.195	.240
34.0	12.5			.066	.070	.070	.065	.061	.061	.065	.069	.073	.080	.075
39.0	12.5			-.015	-.015	-.017	-.023	-.030	-.032	-.036	-.039	-.042	-.045	-.049
49.0	12.5			-.033	-.035	-.043	-.062	-.088	-.097	-.094	-.090	-.090	-.090	-.091
59.0	12.5			-.018	-.015	-.015	-.019	-.024	-.030	-.035	-.040	-.043	-.044	-.045
19.0	17.5			0	0	0	0	0	0	.009	.032	.067	.105	.138
24.0	17.5			.005	.005	.019	.052	.094	.130	.160	.183	.198	.210	.220
26.5	17.5			.025	.031	.085	.126	.152	.169	.189	.206	.218	.225	.222
31.5	17.5			.090	.116	.133	.144	.149	.152	.147	.130	.100	.081	.069
36.5	17.5			.093	.097	.099	.098	.092	.082	.070	.063	.060	.060	.065
41.5	17.5			.025	.029	.030	.025	.017	.010	.007	.005	.005	.005	.005
61.5	17.5			-.037	-.041	-.050	-.049	-.053	-.057	-.061	-.067	-.068	-.072	-.075
31.5	25.0			.005	.008	.020	.040	.066	.085	.095	.103	.107	.110	.110
39.0	25.0			.036	.070	.090	.100	.106	.107	.107	.105	.104	.100	.090
54.0	25.0			.012	.015	.018	.014	.006	-.002	-.006	-.005	-.006	-.006	-.006
59.0	25.0			-.008	-.005	-.009	-.016	-.023	-.025	-.026	-.029	-.030	-.030	-.030
64.0	25.0			-.026	-.027	-.035	-.042	-.048	-.050	-.055	-.056	-.057	-.057	-.054
41.5	30.0			.025	.020	.038	.055	.067	.074	.075	.075	.075	.071	.066
46.5	30.0			.050	.063	.073	.078	.078	.078	.078	.078	.076	.075	.073
51.5	30.0			.035	.035	.046	.055	.055	.055	.050	.049	.043	.035	.025
61.5	30.0			.008	.013	.015	.015	.009	.004	0	-.004	-.005	-.006	-.006

TABLE 5.- WING PRESSURES FOR SUPERSONIC NOZZLE ($M_j = 1.74$) AT POSITION B

x/D_T	y/D_T	10	20	30	40	50	60	70	80	90	100	110	120	130
						Incremental wing pressure coefficients for $p_{t,c}/P_\infty$ of -								
11.5	2.5			0	0	0	0	0	0.002	0.007	0.015	0.028	0.040	
14.0	2.5			.006	.010	.013	.022	.048	.092	.145	.199	.241	.267	
19.0	2.5			.160	.215	.272	.324	.358	.382	.400	.414	.425	.435	
21.5	2.5			.285	.300	.320	.337	.344	.350	.359	.368	.370	.370	
24.0	2.5			.195	.194	.196	.200	.202	.204	.205	.205	.205	.205	
26.5	2.5			.090	.079	.078	.076	.075	.075	.075	.074	.073	.073	
29.0	2.5			-.005	-.010	-.011	-.013	-.015	-.015	-.015	-.015	-.015	-.015	
34.0	2.5			-.115	-.118	-.124	-.137	-.142	-.145	-.149	-.150	-.152	-.153	
39.0	2.5			-.027	-.039	-.039	-.040	-.049	-.055	-.067	-.082	-.015	-.119	
44.0	2.5			-.015	-.018	-.028	-.026	-.020	-.023	-.029	-.034	-.035	-.039	
49.0	2.5			-.013	-.013	-.015	-.016	-.017	-.018	-.019	-.020	-.020	-.020	
54.0	2.5			-.015	-.016	-.017	-.018	-.020	-.020	-.020	-.020	-.021	-.021	
64.0	2.5			-.015	-.015	-.015	-.015	-.015	-.015	-.015	-.015	-.015	-.015	
11.5	7.5			0	0	0	0	0	0	0	0	0	0	
14.0	7.5			0	0	0	0	0	.015	.045	.096	.139	.166	
19.0	7.5			.150	.160	.188	.218	.248	.277	.307	.335	.369	.392	
21.5	7.5			.185	.220	.257	.300	.341	.381	.420	.455	.485	.509	
24.0	7.5			.250	.260	.285	.310	.325	.331	.339	.345	.349	.350	
26.5	7.5			.071	.072	.072	.072	.072	.072	.071	.069	.065	.060	
31.5	7.5			-.022	-.030	-.035	-.040	-.046	-.051	-.057	-.061	-.066	-.066	
36.5	7.5			-.105	-.107	-.108	-.115	-.121	-.126	-.131	-.137	-.143	-.150	
41.5	7.5			-.028	-.025	-.029	-.046	-.073	-.100	-.118	-.125	-.125	-.125	
46.5	7.5			-.018	-.018	-.019	-.020	-.020	-.021	-.022	-.023	-.030	-.045	
51.5	7.5			-.004	-.009	-.010	-.011	-.010	-.010	-.007	-.005	-.003	0	
61.5	7.5			-.013	-.014	-.014	-.015	-.015	-.015	-.015	-.015	-.016	-.016	
9.0	12.5			0	0	0	0	0	0	0	0	0	0	
16.5	12.5			0	0	0	.007	.035	.080	.123	.150	.172	.187	
19.0	12.5			.040	.020	.064	.110	.145	.167	.175	.176	.170	.160	
21.5	12.5			.137	.170	.200	.217	.220	.218	.217	.225	.247	.280	
24.0	12.5			.095	.110	.122	.136	.153	.173	.200	.232	.272	.335	
26.5	12.5			.118	.145	.168	.190	.212	.235	.258	.279	.295	.310	
29.0	12.5			.100	.120	.135	.145	.153	.157	.159	.160	.159	.155	
34.0	12.5			.031	.025	.021	.017	.012	.005	-.002	-.009	-.014	-.017	
39.0	12.5			-.060	-.062	-.065	-.067	-.070	-.079	-.086	-.092	-.096	-.100	
49.0	12.5			-.015	-.017	-.019	-.023	-.032	-.050	-.065	-.080	-.092	-.102	
59.0	12.5			0	-.005	-.007	-.006	-.005	-.005	-.005	-.004	-.003	-.002	
19.0	17.5			.002	.003	.005	.008	.034	.090	.141	.171	.190	.202	
24.0	17.5			.058	.069	.097	.123	.133	.135	.132	.125	.113	.100	
26.5	17.5			.092	.100	.115	.120	.120	.117	.115	.120	.126	.145	
31.5	17.5			.093	.095	.098	.100	.107	.115	.128	.140	.150	.175	
36.5	17.5			.042	.047	.054	.059	.062	.064	.065	.065	.065	.063	
41.5	17.5			-.003	-.005	-.008	-.010	-.014	-.017	-.020	-.025	-.029	-.032	
61.5	17.5			-.011	-.012	-.012	-.012	-.013	-.012	-.011	-.010	-.010	-.010	
31.5	25.0			.075	.080	.094	.099	.116	.120	.123	.125	.125	.126	
39.0	25.0			.066	.073	.075	.075	.075	.074	.070	.065	.060	.055	
54.0	25.0			-.025	-.024	-.020	-.019	-.027	-.035	-.035	-.036	-.036	-.035	
59.0	25.0			-.045	-.040	-.034	-.041	-.049	-.050	-.052	-.054	-.055	-.056	
64.0	25.0			-.022	-.020	-.021	-.024	-.027	-.035	-.038	.042	-.045	-.045	
41.5	30.0			.088	.083	.080	.085	.092	.094	.094	.091	.090	.090	
46.5	30.0			.056	.055	.055	.056	.058	.059	.055	.054	.059	.080	
51.5	30.0			.030	.031	.030	.029	.025	.026	.021	.019	.019	.018	
61.5	30.0			-.033	-.034	-.030	-.025	-.024	-.028	-.030	-.034	-.035	-.035	

TABLE 6.- WING PRESSURES FOR SUPERSONIC NOZZLE ($M_j = 1.74$) AT POSITION C

Orifice ordinates		Incremental wing pressure coefficients for $P_{t,c}/P_\infty$ of -												
x/D_T	y/D_T	10	20	30	40	50	60	70	80	90	100	110	120	130
11.5	2.5	0.005	0.005	0.005	0.006	0.008	0.020	0.050	0.090	0.116	0.145			
14.0	2.5	0	0	0	.025	.085	.125	.170	.255	.310	.345			
19.0	2.5	.159	.240	.255	.265	.269	.275	.280	.277	.275	.273			
21.5	2.5	.140	.150	.154	.160	.165	.163	.160	.155	.150	.151			
24.0	2.5	.080	.084	.085	.085	.088	.085	.081	.075	.073	.071			
26.5	2.5	.010	.011	.013	.013	.010	.007	.004	.001	-.001	-.002			
29.0	2.5	-.033	-.035	-.036	-.037	-.040	-.044	-.047	-.050	-.052	-.053			
34.0	2.5	-.068	-.073	-.078	-.082	-.093	-.100	-.103	-.108	-.108	-.110			
39.0	2.5	-.025	-.025	-.025	-.024	-.029	-.042	-.080	-.107	-.125	-.142			
44.0	2.5	-.020	-.019	-.018	-.017	-.021	-.029	-.030	-.041	-.035	-.038			
49.0	2.5													
54.0	2.5	-.007	-.006	-.005	-.005	-.005	-.005	-.005	-.008	-.007	-.007			
64.0	2.5	-.005	-.005	-.005	-.005	-.005	-.005	-.005	-.005	-.005	-.005			
11.5	7.5	0	0	0	0	0	.002	.005	.007	.020	.057			
14.0	7.5	0	0	0	0	.013	.060	.128	.191	.235	.271			
19.0	7.5	.105	.160	.202	.231	.262	.274	.287	.289	.301	.307			
21.5	7.5	.123	.183	.197	.202	.207	.209	.214	.217	.217	.219			
24.0	7.5	.116	.122	.122	.122	.124	.124	.127	.120	.122	.127			
26.5	7.5	.025	.025	.025	.025	.025	.023	.021	.019	.017	.016			
31.5	7.5	-.036	-.039	-.041	-.044	-.047	-.055	-.062	-.066	-.070	-.071			
36.5	7.5	-.054	.057	-.061	-.072	-.075	-.088	-.092	-.095	-.099	-.102			
41.5	7.5	-.020	-.020	-.020	-.022	-.043	-.071	-.091	-.106	-.100	-.104			
46.5	7.5	-.014	-.015	-.015	-.015	-.018	-.025	-.027	-.026	-.023	-.025			
51.5	7.5	-.010	-.010	-.010	-.010	-.013	-.019	-.019	-.019	-.015	-.015			
61.5	7.5	-.007	-.007	-.006	-.005	-.005	-.006	-.005	-.007	-.007	-.007			
9.0	12.5	0	0	0	0	0	0	0	0	0	0			
16.5	12.5	0	0	0	0	0	.045	.105	.155	.180	.205			
19.0	12.5	0	0	.005	.055	.154	.195	.225	.255	.280	.297			
21.5	12.5	.079	.126	.164	.198	.234	.249	.260	.265	.279	.289			
24.0	12.5	.098	.153	.181	.193	.195	.197	.195	.193	.193	.197			
26.5	12.5	.110	.129	.120	.127	.124	.119	.117	.113	.110	.109			
29.0	12.5	.070	.067	.062	.065	.060	.057	.051	.045	.045	.042			
34.0	12.5	-.016	-.019	-.020	-.026	-.032	-.040	-.045	-.050	-.055	-.056			
39.0	12.5	-.035	-.044	-.050	-.060	-.069	-.075	-.078	-.085	-.086	-.089			
49.0	12.5	-.003	-.005	-.006	-.007	-.015	-.025	-.043	-.067	-.081	-.090			
59.0	12.5	-.010	-.010	-.010	-.010	-.012	-.013	-.013	-.016	-.014	-.013			
19.0	17.5	0	0	0	0	.017	.044	.080	.105	.119	.130			
24.0	17.5	.020	.040	.070	.101	.136	.150	.165	.175	.190	.209			
26.5	17.5	.053	.096	.125	.142	.155	.160	.167	.174	.180	.189			
31.5	17.5	.079	.094	.094	.098	.096	.094	.089	.084	.082	.080			
36.5	17.5	.026	.023	.021	.021	.015	.014	.007	0	-.005	-.007			
41.5	17.5	-.035	-.036	-.035	-.039	-.045	-.050	-.053	-.057	-.062	-.065			
61.5	17.5	-.005	-.007	-.009	-.010	-.012	-.014	-.015	-.015	-.016	-.016			
31.5	25.0	-----	-----	-----	-----	-----	-----	-----	-----	-----	-----			
39.0	25.0	.053	.068	.069	.074	.074	.070	.068	.065	.065	.066			
54.0	25.0	-.043	-.040	-.031	-.027	-.030	-.044	-.049	-.050	-.050	-.050			
59.0	25.0	-.045	-.043	-.040	-.035	-.041	-.050	-.050	-.051	-.052	-.052			
64.0	25.0	-----	-----	-----	-----	-----	-----	-----	-----	-----	-----			
41.5	30.0	-----	-----	-----	-----	-----	-----	-----	-----	-----	-----			
46.5	30.0	.045	.050	.048	.045	.045	.046	.045	.045	.045	.045			
51.5	30.0	-----	-----	-----	-----	-----	-----	-----	-----	-----	-----			
61.5	30.0	-.010	-.018	-.025	-.030	-.033	-.035	-.035	-.036	-.038	-.040			

TABLE 7.- WING PRESSURES FOR SUPERSONIC NOZZLE ($M_j = 3.04$) AT POSITION A

Orifice ordinates		Incremental wing pressure coefficients for $p_{t,c}/p_\infty$ of -												
x/D_T	y/D_T	10	20	30	40	50	60	70	80	90	100	110	120	130
11.5	2.5	0	0	0	0	0	0	0	0	0	0			
14.0	2.5	0	0	0	0	0	0	0	0	0	0			
19.0	2.5	.005	.015	.001	.015	.042	.061	.074	.106	.160	.246			
21.5	2.5	.003	.023	.043	.071	.156	.383	.459	.488	.488	.471			
24.0	2.5	.115	.277	.435	.586	.525	.506	.495	.494	.490	.500			
26.5	2.5	.211	.439	.385	.325	.287	.257	.240	.210	.195	.190			
29.0	2.5	0	0	0	-.027	-.065	-.085	-.100	-.115	-.130	-.140			
34.0	2.5	-.050	-.097	-.137	-.168	-.193	-.208	-.220	-.230	-.245	-.254			
39.0	2.5	-.003	-.012	-.025	-.040	-.059	-.077	-.095	-.112	-.127	-.140			
44.0	2.5	-.007	-.012	-.018	-.026	-.038	-.055	-.070	-.083	-.090	-.095			
49.0	2.5	-----	-----	-----	-----	-----	-----	-----	-----	-----	-----			
54.0	2.5	-.005	-.007	-.009	-.010	-.014	-.017	-.019	-.020	-.023	-.025			
64.0	2.5	-.002	-.002	-.005	-.008	-.010	-.014	-.014	-.012	-.011	-.010			
11.5	7.5	0	0	0	0	0	0	0	0	0	0			
14.0	7.5	.004	.004	.004	.004	-.001	-.006	-.006	-.006	-.006	-.006			
19.0	7.5	0	.003	.005	.009	.043	.098	.150	.195	.230	.252			
21.5	7.5	.007	.020	.066	.141	.204	.247	.277	.299	.324	.348			
24.0	7.5	.036	.126	.206	.265	.300	.323	.348	.371	.393	.416			
26.5	7.5	.040	.070	.085	.095	.107	.129	.155	.200	.244	.265			
31.5	7.5	.007	.022	.042	.069	.112	.160	.165	.075	-.020	-.100			
36.5	7.5	-.025	-.045	-.062	-.070	-.077	-.084	-.100	-.130	-.172	-.225			
41.5	7.5	-.020	-.042	-.065	-.087	-.110	-.128	-.146	-.162	-.175	-.182			
46.5	7.5	-.012	-.017	-.016	-.018	-.026	-.039	-.050	-.059	-.062	-.065			
51.5	7.5	-.011	-.017	-.019	-.019	-.020	-.025	-.026	-.026	-.025	-.022			
61.5	7.5	-.005	-.017	-.017	-.017	-.017	-.019	-.020	-.020	-.020	-.020			
9.0	12.5	0	0	0	0	0	0	0	0	0	0			
16.5	12.5	0	0	0	0	0	0	0	0	0	0			
19.0	12.5	0	0	0	0	0	0	0	.025	.064	.112			
21.5	12.5	0	0	0	.005	.030	.092	.142	.184	.216	.242			
24.0	12.5	.012	.020	.033	.095	.165	.198	.220	.242	.261	.280			
26.5	12.5	.015	.056	.118	.164	.192	.213	.228	.239	.246	.253			
29.0	12.5	.034	.090	.134	.157	.170	.179	.185	.190	.192	.195			
34.0	12.5	.050	.076	.075	.074	.075	.075	.077	.085	.099	.115			
39.0	12.5	.018	.005	-.009	-.015	-.019	-.025	-.026	-.028	-.030				
49.0	12.5	-.017	-.030	-.040	-.049	-.064	-.084	-.102	-.114	-.122	-.128			
59.0	12.5	-.006	-.011	-.014	-.015	-.016	-.020	-.022	-.026	-.030	-.035			
19.0	17.5	0	0	0	0	0	0	0	0	0	.010			
24.0	17.5	0	0	.004	.005	.010	.034	.074	.114	.147	.162			
26.5	17.5	0	.004	.005	.025	.076	.118	.147	.170	.185	.196			
31.5	17.5	.006	.035	.077	.111	.130	.144	.150	.152	.155	.155			
36.5	17.5	.022	.059	.085	.095	.095	.095	.094	.091	.088	.085			
41.5	17.5	.012	.025	.024	.021	.020	.018	.015	.010	.009	.008			
61.5	17.5	-.007	-.011	-.015	-.020	-.023	-.027	-.031	-.035	-.039	-.044			
31.5	25.0													
39.0	25.0	.005	.020	.043	.065	.085	.095	.103	.105	.108	.108			
54.0	25.0	.007	.012	.015	.015	.014	.011	.009	.004	0	-.005			
59.0	25.0	-.006	-.012	-.015	-.018	-.020	-.023	-.025	-.026	-.027	-.030			
64.0	25.0													
41.5	30.0													
46.5	30.0	.028	.045	.055	.060	.072	.078	.083	.084	.086	.086			
51.5	30.0													
61.5	30.0	.010	.015	.015	.015	.013	.009	.005	0	0	0			

TABLE 8.- WING PRESSURES FOR SUPERSONIC NOZZLE ($M_j = 3.04$) AT POSITION C

Orifice ordinates		Incremental wing pressure coefficients for $p_{t,c}/P_\infty$ of -												
x/D_T	y/D_T	10	20	30	40	50	60	70	80	90	100	110	120	130
11.5	2.5	0	0	0	.005	.005	.005	.005	.011	.028	.066	.116	.158	.188
14.0	2.5	0	0	0	.005	.016	.042	.110	.175	.229	.280	.325	.370	.410
19.0	2.5	.057	.116	.175	.228	.268	.287	.301	.315	.324	.328	.327	.325	.320
21.5	2.5	.100	.147	.178	.200	.207	.205	.205	.205	.204	.199	.194	.191	
24.0	2.5	.090	.107	.115	.115	.115	.115	.113	.111	.109	.106	.101	.100	.100
26.5	2.5	.058	.060	.060	.055	.054	.050	.048	.045	.040	.035	.033	.030	.027
29.0	2.5	.011	.013	.007	-.001	-.007	-.010	-.015	-.017	-.020	-.025	-.027	-.030	-.035
34.0	2.5	-.040	-.064	-.077	-.085	-.087	-.090	-.094	-.095	-.097	-.100	-.098	-.100	-.100
39.0	2.5	-.016	-.018	-.024	-.027	-.047	-.098	-.115	-.126	-.135	-.143	-.146	-.149	-.150
44.0	2.5	-.014	-.020	-.024	-.024	-.025	-.026	-.030	-.033	-.035	-.040	-.048	-.057	-.068
49.0	2.5	-.010	-.013	-.017	-.020	-.025	-.027	-.030	-.033	-.035	-.035	-.036	-.038	-.040
54.0	2.5	-.009	-.010	-.012	-.012	-.010	-.010	-.010	-.008	-.007	-.010	-.015	-.017	-.020
64.0	2.5	-.005	-.005	-.005	-.005	-.005	-.005	-.005	-.005	-.005	-.005	-.005	-.005	-.005
11.5	7.5	.005	.007	.007	.007	.007	.007	.007	.007	.007	.006	.022	.052	.113
14.0	7.5	.004	.006	.007	.007	.006	.005	.032	.090	.162	.210	.250	.285	.315
19.0	7.5	.038	.076	.133	.220	.273	.300	.315	.326	.337	.345	.350	.356	.357
21.5	7.5	.068	.150	.200	.227	.238	.241	.245	.245	.247	.247	.245	.245	.245
24.0	7.5	.112	.148	.155	.159	.160	.160	.155	.154	.150	.146	.143	.138	.133
26.5	7.5	.026	.030	.032	.032	.032	.030	.029	.026	.025	.020	.019	.016	.015
31.5	7.5	-.010	-.017	-.021	-.025	-.027	-.031	-.035	-.040	-.044	-.048	-.054	-.057	-.060
36.5	7.5	-.055	-.066	-.072	-.083	-.090	-.096	-.100	-.105	-.107	-.110	-.113	-.115	-.116
41.5	7.5	-.014	-.015	-.017	-.019	-.042	-.087	-.105	-.111	-.118	-.124	-.125	-.125	-.125
46.5	7.5	-.014	-.015	-.018	-.022	-.024	-.025	-.025	-.026	-.036	-.063	-.090	-.109	-.115
51.5	7.5	-.011	-.015	-.013	-.013	-.013	-.014	-.014	-.015	-.015	-.015	-.016	-.018	-.020
61.5	7.5	-.004	-.004	-.004	-.004	-.004	-.004	-.004	-.004	-.004	-.004	-.004	-.004	-.004
9.0	12.5	0	0	0	0	0	0	0	0	0	0	0	0	0
16.5	12.5	0	0	0	0	0	.005	.041	.102	.148	.176	.198	.220	.240
19.0	12.5	0	.002	.003	.013	.094	.165	.209	.235	.262	.289	.316	.343	.370
21.5	12.5	.028	.050	.087	.162	.218	.248	.270	.289	.303	.316	.325	.336	.346
24.0	12.5	.070	.132	.182	.207	.220	.226	.231	.235	.235	.236	.235	.235	.234
26.5	12.5	.097	.143	.154	.155	.152	.153	.150	.145	.143	.140	.136	.132	.128
29.0	12.5	.085	.090	.087	.083	.077	.073	.068	.064	.060	.059	.056	.055	.051
34.0	12.5	.011	.005	-.001	-.005	-.010	-.016	-.020	-.025	-.029	-.033	-.036	-.040	-.045
39.0	12.5	-.044	-.051	-.055	-.060	-.064	-.067	-.072	-.075	-.078	-.081	-.084	-.086	-.089
49.0	12.5	-.005	-.007	-.010	-.011	-.012	-.020	-.050	-.074	-.089	-.103	-.115	-.123	-.125
59.0	12.5	-.005	-.005	-.005	-.005	-.005	-.005	-.005	-.005	-.005	-.005	-.005	-.005	-.005
19.0	17.5	0	0	0	.002	.004	.025	.062	.094	.116	.132	.142	.150	.155
24.0	17.5	.002	.007	.015	.080	.125	.146	.162	.181	.200	.221	.243	.265	.287
26.5	17.5	.022	.052	.092	.138	.154	.167	.180	.191	.205	.214	.221	.227	.231
31.5	17.5	.065	.100	.106	.109	.109	.108	.105	.103	.100	.098	.094	.090	.086
36.5	17.5	.045	.040	.035	.030	.025	.020	.015	.012	.009	.005	.003	0	-.004
41.5	17.5	-.023	-.030	-.037	-.044	-.050	-.055	-.056	-.060	-.063	-.065	-.069	-.071	-.075
61.5	17.5	-.004	-.005	-.005	-.005	-.006	-.007	-.010	-.011	-.016	-.025	-.033	-.040	-.050
31.5	25.0	.025	.025	.030	.058	.098	.110	.106	.109	.120	.125	.130	.131	.133
39.0	25.0	.045	.072	.080	.078	.079	.077	.076	.075	.075	.075	.075	.075	.075
54.0	25.0	-.015	-.024	-.030	-.035	-.039	-.042	-.045	-.050	-.055	-.058	-.059	-.060	-.060
59.0	25.0	-.010	-.021	-.030	-.042	-.049	-.055	-.058	-.060	-.060	-.060	-.060	-.060	-.060
64.0	25.0	-.014	-.016	-.015	-.017	-.020	-.024	-.031	-.040	-.045	-.047	-.049	-.050	-.050
41.5	30.0	.025	.035	.056	.074	.075	-.075	-.075	.074	.071	.070	.070	.070	.070
46.5	30.0	.050	.052	.052	.052	.050	.050	.050	.049	.048	.046	.045	.045	.044
51.5	30.0	.015	.015	.014	.017	.020	.017	.013	.010	.005	.004	0	0	0
61.5	30.0	-.024	-.025	-.029	-.033	-.035	-.040	-.045	-.046	-.047	-.049	-.050	-.050	-.050

TABLE 9.- WING PRESSURES FOR TWO-DIMENSIONAL SUPERSONIC NOZZLE (M_J = 1.71) AT POSITION A

Orifice ordinates		Incremental wing pressure coefficients for $p_{t,c}/p_\infty$ of -												
x/D_T	y/D_T	10	20	30	40	50	60	70	80	90	100	110	120	130
11.5	2.5	0	0	0	0	0	0							
14.0	2.5	0	0	0	0	0	0							
19.0	2.5	.008	.035	.075	.120	.162	.208							
21.5	2.5	.058	.145	.207	.261	.310	.355							
24.0	2.5	.175	.303	.390	.412	.525	.588							
26.5	2.5	.220	.300	.330	.328	.326	.325							
29.0	2.5	.025	.020	-.006	-.040	-.075	-.114							
34.0	2.5	-.082	-.130	-.160	-.186	-.243	-.260							
39.0	2.5	-.036	-.045	-.047	-.050	-.055	-.056							
44.0	2.5	-.024	-.031	-.030	-.034	-.043	-.055							
49.0	2.5	-.023	-.030	-.034	-.037	-.040	-.040							
54.0	2.5	-.016	-.020	-.020	-.025	-.033	-.036							
64.0	2.5	-.005	-.008	-.009	-.013	-.015	-.020							
11.5	7.5	-.005	-.006	-.006	-.005	-.005	-.005							
14.0	7.5	-.010	-.010	-.010	-.010	-.010	-.010							
19.0	7.5	-.014	-.013	-.010	.011	.065	.141							
21.5	7.5	-.010	.022	.088	.150	.192	.227							
24.0	7.5	.052	.140	.186	.202	.250	.279							
26.5	7.5	.013	.054	.076	.090	.105	.128							
31.5	7.5	.088	.088	.090	.105	.121	.115							
36.5	7.5	-.080	-.085	-.085	-.082	-.094	-.112							
41.5	7.5	-.055	-.075	-.087	-.104	-.130	-.171							
46.5	7.5	-.018	-.023	-.021	-.019	-.025	-.036							
51.5	7.5	-.025	-.030	-.030	-.035	-.039	-.042							
61.5	7.5	-.010	-.015	-.020	-.024	-.030	-.035							
9.0	12.5	0	0	0	0	0	0							
16.5	12.5	0	0	0	0	0	0							
19.0	12.5	0	0	0	0	0	.015							
21.5	12.5	0	0	0	.021	.086	.156							
24.0	12.5	.002	.025	.068	.123	.158	.184							
26.5	12.5	.050	.106	.127	.142	.154	.163							
29.0	12.5	.086	.121	.125	.125	.125	.125							
34.0	12.5	.082	.087	.084	.091	.105	.122							
39.0	12.5	.020	.013	.011	.010	.012	.015							
49.0	12.5	-.028	-.046	-.052	-.055	-.065	-.080							
59.0	12.5	-.010	-.014	-.015	-.020	-.025	-.030							
19.0	17.5	0	0	0	0	0	0							
24.0	17.5	0	0	0	.010	.054	.118							
26.5	17.5	0	0	.024	.070	.109	.138							
31.5	17.5	.018	.060	.093	.105	.102	.099							
36.5	17.5	.040	.068	.071	.066	.060	.050							
41.5	17.5	0	0	0	0	0	0							
61.5	17.5	-.007	-.012	-.017	-.020	-.020	-.021							
31.5	25.0	0	.002	.005	.025	.076	.016							
39.0	25.0	.009	.037	.052	.065	.070	.075							
54.0	25.0	.005	.008	.009	.007	.005	.002							
59.0	25.0	-.010	-.015	-.017	-.020	-.021	-.023							
64.0	25.0	-.015	-.023	-.027	-.031	-.035	-.035							
41.5	30.0	.010	.022	.035	.056	.074	.086							
46.5	30.0	.027	.044	.050	.060	.065	.066							
51.5	30.0	.030	.035	.042	.044	.043	.039							
61.5	30.0	.003	.005	.005	.003	-.002	-.006							

TABLE 10.- WING PRESSURES FOR TWO-DIMENSIONAL SUPERSONIC NOZZLE (M_j = 1.71) AT POSITION B

Orifice ordinates		Incremental wing pressure coefficients for $p_{t,c}/P_\infty$ of -												
x/D_T	y/D_T	10	20	30	40	50	60	70	80	90	100	110	120	130
11.5	2.5	0	0	0	0	0	0							
14.0	2.5	0	0	0	.015	.044	.080							
19.0	2.5	0	.082	.182	.280	.355	.420							
21.5	2.5	.065	.160	.325	.306	.280	.295							
24.0	2.5	.114	.142	.148	.153	.156	.152							
26.5	2.5	.050	.050	.038	.032	.024	.015							
29.0	2.5	-.003	-.022	-.034	-.041	-.050	-.056							
34.0	2.5	-.021	-.055	-.085	-.107	-.125	-.137							
39.0	2.5	-.014	-.030	-.035	-.032	-.046	-.040							
44.0	2.5	-.012	-.018	-.020	-.021	-.021	-.018							
49.0	2.5	-.011	-.013	-.014	-.015	-.015	-.016							
54.0	2.5	-.006	0	-.008	-.011	-.010	-.006							
64.0	2.5	.006	0	-.009	-.010	-.012	-.015							
11.5	7.5	0	0	0	0	0	0							
14.0	7.5	0	0	0	0	0	0							
19.0	7.5	0	.017	.115	.203	.260	.306							
21.5	7.5	.018	.120	.224	.279	.314	.338							
24.0	7.5	.062	.166	.230	.244	.249	.251							
26.5	7.5	.034	.047	.048	.049	.049	.045							
31.5	7.5	0	-.006	-.024	-.039	-.049	-.056							
36.5	7.5	-.033	-.076	-.105	-.107	-.110	-.126							
41.5	7.5	-.007	-.020	-.026	-.031	-.041	-.051							
46.5	7.5	0	-.011	-.021	-.026	-.029	-.030							
51.5	7.5	0	0	0	-.001	-.005	-.006							
61.5	7.5	-.002	-.005	-.010	-.012	-.013	-.015							
9.0	12.5	0	0	0	0	0	0							
16.5	12.5	0	0	0	0	0	0							
19.0	12.5	0	0	0	.003	.060	.137							
21.5	12.5	0	0	.056	.135	.197	.230							
24.0	12.5	0	.077	.163	.210	.240	.259							
26.5	12.5	.015	.125	.185	.204	.217	.223							
29.0	12.5	.050	.108	.130	.133	.135	.135							
34.0	12.5	.041	.028	.016	.007	-.002	-.013							
39.0	12.5	-.023	-.040	-.051	-.054	-.059	-.065							
49.0	12.5	0	-.015	-.025	-.030	-.040	-.055							
59.0	12.5	-.009	-.014	-.015	-.015	-.014	-.012							
19.0	17.5	0	0	0	0	0	.005							
24.0	17.5	0	0	.010	.054	.111	.136							
26.5	17.5	0	.007	.077	.132	.156	.169							
31.5	17.5	.020	.095	.125	.133	.140	.145							
36.5	17.5	.055	.069	.066	.062	.060	.056							
41.5	17.5	.023	.011	0	-.003	-.010	-.018							
61.5	17.5	0	-.007	-.015	-.017	-.020	-.023							
31.5	25.0	.007	.015	.025	.047	.073	.090							
39.0	25.0	.005	.053	.082	.087	.090	.092							
54.0	25.0	.017	.018	.010	-.007	-.019	-.021							
59.0	25.0	-.011	-.026	-.035	-.040	-.045	-.050							
64.0	25.0	-.025	-.034	-.030	-.025	-.025	-.033							
41.5	30.0	.060	.070	.070	.070	.075	.080							
46.5	30.0	.028	.048	.059	.065	.067	.070							
51.5	30.0	.023	.029	.030	.032	.030	.019							
61.5	30.0	.009	.002	-.003	-.007	-.009	-.015							

TABLE 11.- VERTICAL-STRUT PRESSURES FOR SONIC NOZZLE

Orifice ordinates		Incremental vertical strut pressure coefficients for $p_{t,c}/p_\infty$ of -											
x/D_T	z/D_T	10	20	30	40	50	60	70	80	90	100	110	120	130
(a) Position A														
29	4.05					-0.216	-0.218	-0.223	-0.240	-0.260	-0.295	-0.317		
39	4.05					-.050	-.093	-.108	-.102	-.082	-.068	-.063		
49	4.05					-.030	-.030	-.030	-.027	-.026	-.028	-.032		
22.25	8.0					.228	.213	.195	.175	.175	.188	.204		
32.25	8.0					-.126	-.141	-.153	-.167	-.181	-.195	-.208		
42.25	8.0					-.066	-.066	-.069	-.075	-.080	-.075	-.065		
15.5	12					0	0	0	0	0	0	0		
25.5	12					.152	.146	.160	.185	.189	.166	.150		
35.5	12					-.025	-.025	-.025	-.025	-.024	-.021	-.020		
(b) Position B														
29	4.05			0.03	-0.042	-0.086	-0.110	-0.120	-0.125	-0.127	-0.127			
39	4.05			-.030	-.040	-.041	-.050	-.051	-.060	-.067	-.065			
49	4.05			-.015	-.015	-.015	-.015	-.017	-.019	-.022	-.032			
22.25	8.0			-.150	-.234	-.252	-.245	-.244	-.250	-.259	-.270			
32.25	8.0			.003	.029	.045	.048	.043	.045	.046	.052			
42.25	8.0			-.021	-.023	-.026	-.031	-.030	-.035	-.035	-.032			
15.5	12			.153	.176	.204	.215	.219	.206	.187	.185			
25.5	12			-.105	-.110	-.142	-.190	-.207	-.214	-.220	-.222			
35.5	12			.025	.017	.012	.015	.024	.029	.029	.029			
(c) Position C														
29	4.05	0.014	-0.001	-0.011	-0.017	-0.020	-0.036	-0.058	-0.066	-0.070	-0.075			
39	4.05	-.032	-.044	-.045	-.047	-.047	-.050	-.057	-.058	-.061	-.070			
49	4.05	-.001	-.003	-.004	-.005	-.008	-.010	-.011	-.014	-.015	-.017			
22.25	8.0	-.017	-.030	-.037	-.045	-.057	-.097	-.120	-.133	-.134	-.140			
32.25	8.0	.023	.025	.025	.025	.025	.024	.023	.020	.015	.010			
42.25	8.0	-.012	-.015	-.017	-.019	-.020	-.023	-.025	-.028	-.030	-.030			
15.5	12	-.144	-.251	-.290	-.302	-.300	-.305	-.318	-.328	-.336	-.345			
25.5	12	-.010	-.015	-.015	-.010	-.009	-.032	-.027	-.007	.010	.025			
35.5	12	.017	.024	.025	.025	.025	.022	.020	.020	.017	.015			

TABLE 12.- VERTICAL-STRUT PRESSURES FOR SUPERSONIC NOZZLE (M = 1.74)

Orifice ordinates		Incremental vertical strut pressure coefficients for $p_{t,c}/p_\infty$ of -												
x/D_T	z/D_T	10	20	30	40	50	60	70	80	90	100	110	120	130
(a) Position A														
29	4.05			-0.189	-0.213	-0.226	-0.231	-0.236	-0.250	-0.268	-0.287	-0.298	-0.305	-0.306
39	4.05			-.040	-.032	-.036	-.049	-.055	-.055	-.056	-.062	-.070	-.080	-.090
49	4.05			-.006	-.006	-.008	-.010	-.010	-.012	-.015	-.018	-.023	-.030	-.040
22.25	8.0			.131	.180	.205	.200	.175	.151	.157	.183	.220	.265	.320
32.25	8.0			-.088	-.107	-.131	-.140	-.156	-.172	-.187	-.195	-.200	-.205	-.206
42.25	8.0			-.020	-.030	-.030	-.022	-.010	-.005	-.004	-.006	-.016	-.027	-.036
15.5	12			-.005	-.005	-.005	-.005	-.005	-.005	-.005	-.005	-.005	-.005	-.005
25.5	12			.110	.115	.138	.141	.135	.115	.101	.105	.120	.150	.182
35.5	12			-.026	-.027	-.027	-.028	-.029	-.030	-.032	-.034	-.036	-.040	-.045
(b) Position B														
29	4.05			-0.010	-0.030	-0.063	-0.104	-0.114	-0.118	-0.122	-0.125	-0.127	-0.128	
39	4.05			-.046	-.050	-.057	-.061	-.066	-.072	-.077	-.083	-.090	-.097	
49	4.05			-.020	-.022	-.025	-.025	-.026	-.027	-.029	-.030	-.031	-.055	
22.25	8.0			-.183	-.205	-.213	-.215	-.220	-.228	-.240	-.260	-.268	-.270	
32.25	8.0			.048	.045	.037	.040	.058	.086	.115	.130	.135	.150	
42.25	8.0			-.027	-.027	-.025	-.025	-.025	-.024	-.022	-.020	-.017	-.014	
15.5	12			.150	.159	.178	.198	.215	.226	.232	.225	.212	.220	
25.5	12			-.125	-.150	-.165	-.178	-.185	-.194	-.200	-.203	-.207	-.210	
35.5	12			.037	.040	.040	.038	.039	.045	.054	.060	.064	.074	
(c) Position C														
29	4.05	0.005	0.005	0.000	-0.012	-0.035	-0.049	-0.057	-0.063	-0.065	-0.065			
39	4.05	-.030	-.035	-.030	-.035	-.045	-.052	-.055	-.055	-.057	-.060			
49	4.05	-.014	-.015	-.015	-.018	-.020	-.020	-.020	-.022	-.024	-.025			
22.25	8.0	-.050	-.065	-.072	-.095	-.125	-.135	-.148	-.150	-.152	-.155			
32.25	8.0	.014	.020	.020	.020	.020	.018	.015	.015	.012	.010			
42.25	8.0	-.010	-.015	-.015	-.015	-.015	-.020	-.020	-.025	-.026	-.030			
15.5	12	-.195	-.236	-.244	-.252	-.267	-.270	-.283	-.292	-.295	-.295			
25.5	12	-.028	-.055	-.035	-.030	-.018	-.015	-.008	.005	.010	.013			
35.5	12	.016	.016	.012	.015	.014	.010	.012	.016	.017	.020			

TABLE 13.- VERTICAL-STRUT PRESSURES FOR SUPERSONIC NOZZLE (M = 3.04)

(a) Position A

Orifice ordinates		Incremental strut pressure coefficients for $p_{t,c}/p_\infty$ of -												
x/D_T	z/D_T	10	20	30	40	50	60	70	80	90	100	110	120	130
29	4.05	-0.010	-0.035	-0.070	-0.120	-0.157	-0.175	-0.187	-0.190	-0.200	-0.213			
39	4.05	-.000	-.001	-.022	-.044	-.040	-.023	-.045	-.080	-.080	-.065			
49	4.05	-.007	-.013	-.017	-.020	-.025	-.025	-.025	-.025	-.022	-.020			
22.25	8.0	.100	.100	.127	.170	.205	.205	.181	.173	.176	.190			
32.25	8.0	-.010	-.030	-.060	-.095	-.124	-.139	-.147	-.157	-.162	-.168			
42.25	8.0	-.015	-.029	-.035	-.035	-.035	-.029	-.027	-.035	-.035	-.035			
15.5	12	-.010	-.010	-.002	-.002	-.002	-.002	-.003	-.004	-.005	-.005			
25.5	12	.008	.040	.090	.124	.135	.140	.140	.142	.135	.123			
35.5	12	-.005	-.008	-.014	-.017	-.021	-.022	-.020	-.021	-.021	-.021			

(b) Position C

Orifice ordinates		Incremental strut pressure coefficients for $p_{t,c}/p_\infty$ of -												
x/D_T	z/D_T	10	20	30	40	50	60	70	80	90	100	110	120	130
29	4.05	0.010	0.000	-0.010	-0.025	-0.038	-0.048	-0.055	-0.059	-0.060	-0.065	-0.065	-0.067	-0.069
39	4.05	-.025	-.032	-.035	-.037	-.040	-.044	-.048	-.053	-.057	-.062	-.067	-.073	-.077
49	4.05	-.008	-.010	-.010	-.012	-.015	-.015	-.015	-.015	-.023	-.029	-.036	-.044	-.050
22.25	8.0	-.030	-.050	-.069	-.086	-.100	-.107	-.110	-.115	-.117	-.120	-.125	-.126	-.130
32.25	8.0	.020	.025	.028	.035	.035	.035	.035	.030	.030	.030	.022	.018	.015
42.25	8.0	-.017	-.020	-.019	-.016	-.016	-.018	-.020	-.024	-.025	-.029	-.032	-.035	-.040
15.5	12	-.127	-.163	-.187	-.205	-.220	-.229	-.237	-.244	-.250	-.256	-.263	-.270	-.275
25.5	12	-.010	-.014	-.013	-.016	-.020	-.018	-.011	-.014	-.025	-.024	-.010	-.016	-.048
35.5	12	.024	.026	.026	.023	.023	.023	.020	.020	.020	.018	.020	.020	.020

TABLE 14.- VERTICAL-STRUT PRESSURES FOR TWO-DIMENSIONAL SUPERSONIC NOZZLE (M = 1.71)

Orifice ordinates		Incremental strut pressure coefficients for $P_{t,c}/p_\infty$ of -												
x/D_T	z/D_T	10	20	30	40	50	60	70	80	90	100	110	120	130
(a) Position A														
29	4.05	-0.070	-0.105	-0.140	-0.198	-0.227	-0.240							
39	4.05	-.018	-.028	-.040	-.052	-.065	-.075							
49	4.05	-.015	-.017	-.020	-.024	-.025	-.030							
22.25	8.0	.064	.145	.170	.163	.148	.135							
32.25	8.0	-.008	-.008	-.025	-.065	-.110	-.142							
42.25	8.0	-.015	-.030	-.040	-.045	-.060	-.080							
15.5	12	-.002	-.005	-.005	-.007	-.010	-.010							
25.5	12	.024	.070	.095	.092	.097	.110							
35.5	12	.004	.001	-.009	-.018	-.024	-.025							
(b) Position B														
29	4.05	0.015	0.008	-0.015	-0.052	-0.085	-0.112							
39	4.05	-.015	-.027	-.038	-.045	-.055	-.060							
49	4.05	-.002	-.004	-.005	-.008	-.010	-.011							
22.25	8.0	-.080	-.125	-.172	-.211	-.235	-.262							
32.25	8.0	.025	.035	.028	.035	.035	.032							
42.25	8.0	-.005	-.010	-.017	-.020	-.025	-.032							
15.5	12	.050	.125	.155	.160	.170	.158							
25.5	12	-.040	-.050	-.076	-.105	-.115	-.118							
35.5	12	-.005	.003	.015	.020	.018	.017							

L-57-836.1

Figure 1.- Typical test setup.
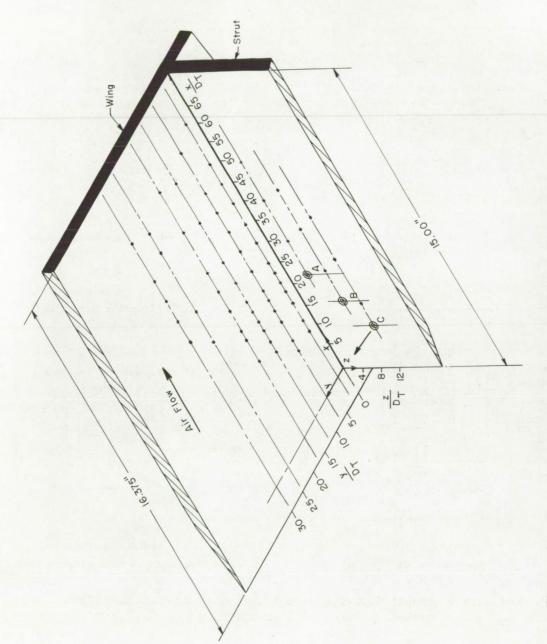
Figure 2.- Three-dimensional drawing of arrangement of flat-plate wing and vertical strut with wing and strut static-pressure orifices and rocket-nozzle position indicated.
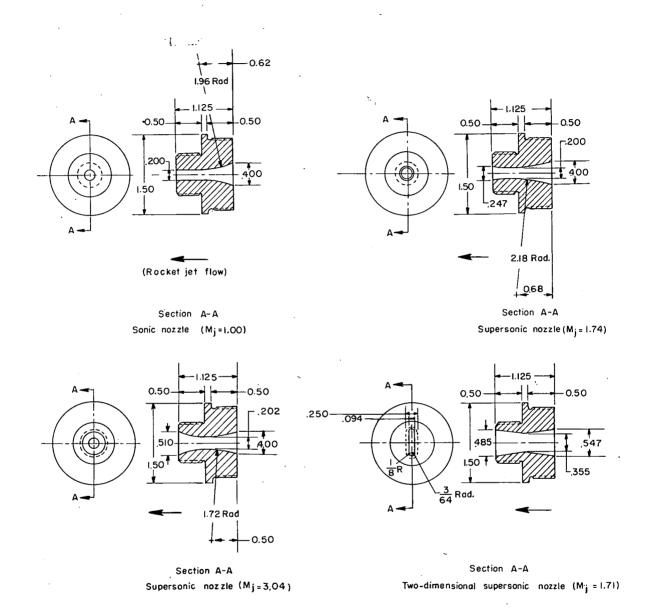
Figure 3.- Nozzle geometries and parameters used in the investigation. $\gamma = 1.25$ for rocket gases. (All dimensions are in inches.)
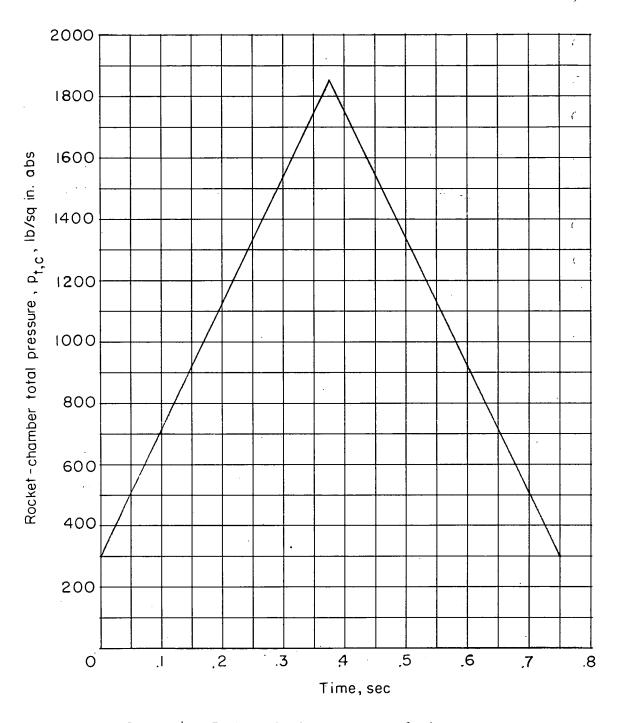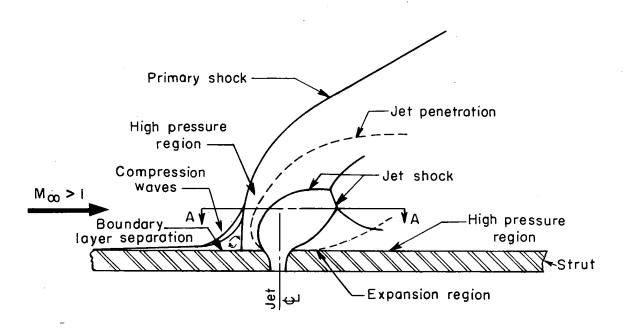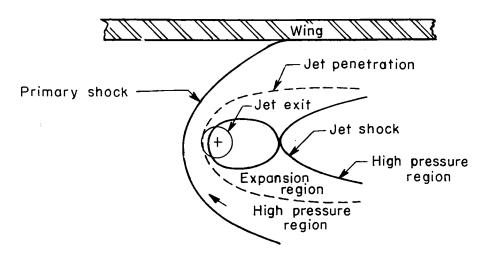
Figure 4.- Rocket-chamber-pressure design curve.

(a) Flow field and nomenclature.

(b) Section A-A of flow field.

Figure 5.- Drawing and nomenclature of the flow field about a jet
exhausting normal to free stream.
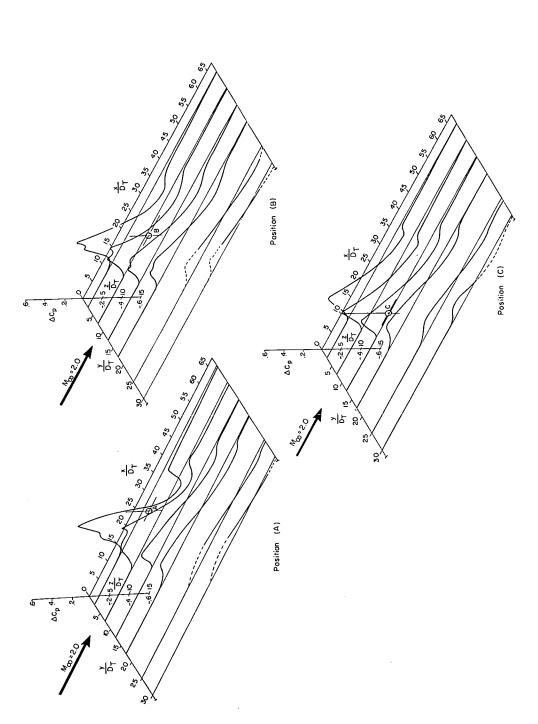
Figure 6.- Variation of chordwise and spanwise incremental pressure coefficient with nozzle position for sonic jet ($M_j = 1.0$) and pressure ratio of 58. Dashed portions of curves indicate omission of pressure measurements.
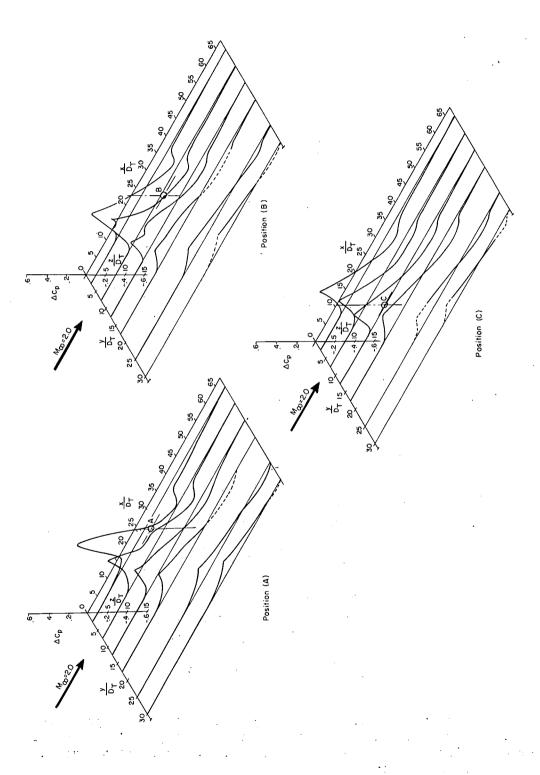
Figure 7.- Variation of chordwise and spanwise incremental pressure coefficient with nozzle position for supersonic jet (M_j = 1.74) and pressure ratio of 58. Dashed portions of curves indicate omission of pressure measurements.
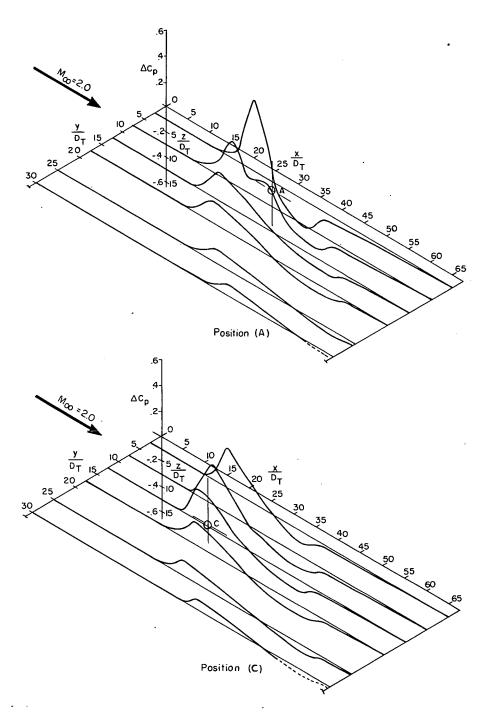
Figure 8.- Variation of chordwise and spanwise incremental pressure
coefficient with nozzle position for supersonic jet (M_j = 3.04) and
pressure ratio of 58. Dashed portions of curves indicate omission
of pressure measurements.
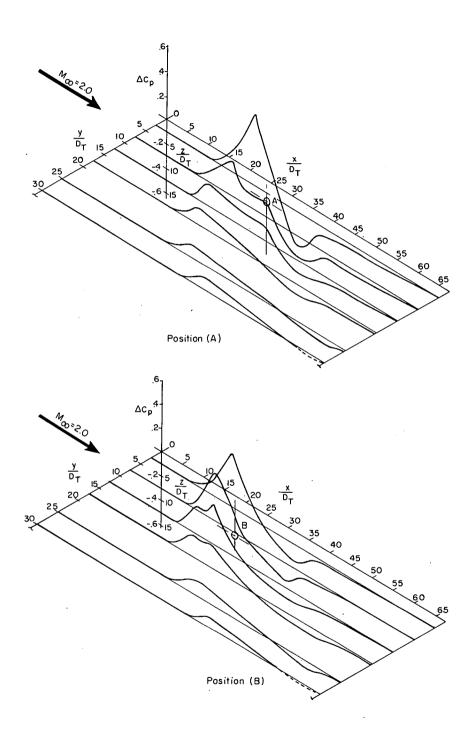
Figure 9.- Variation of chordwise and spanwise incremental pressure
coefficient with nozzle position for two-dimensional supersonic jet
$(M_j = 1.71)$ and pressure ratio of 58. Dashed portions of curves
indicate omission of pressure measurements.
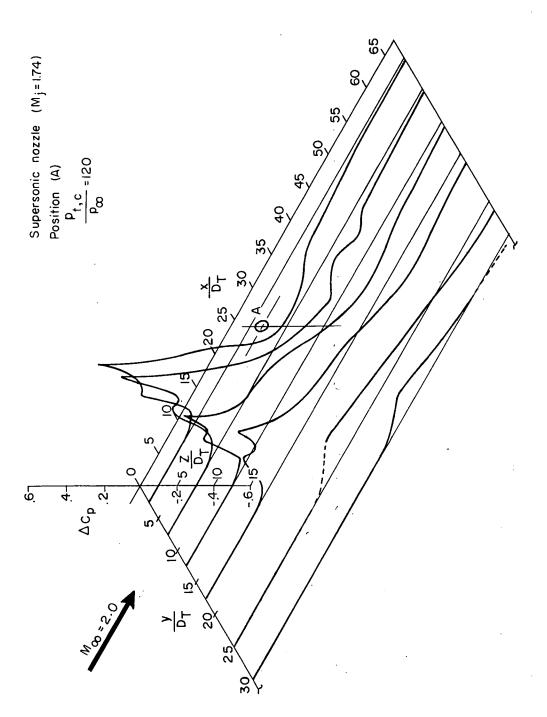
Figure 10.- Chordwise and spanwise incremental pressure coefficient for supersonic nozzle ($M_j = 1.74$) in position A and for pressure ratio of 120. Dashed portions of curves indicate omission of pressure measurements.

(a) Effect of rocket-nozzle position.

(b) Effect of rocket-nozzle type.
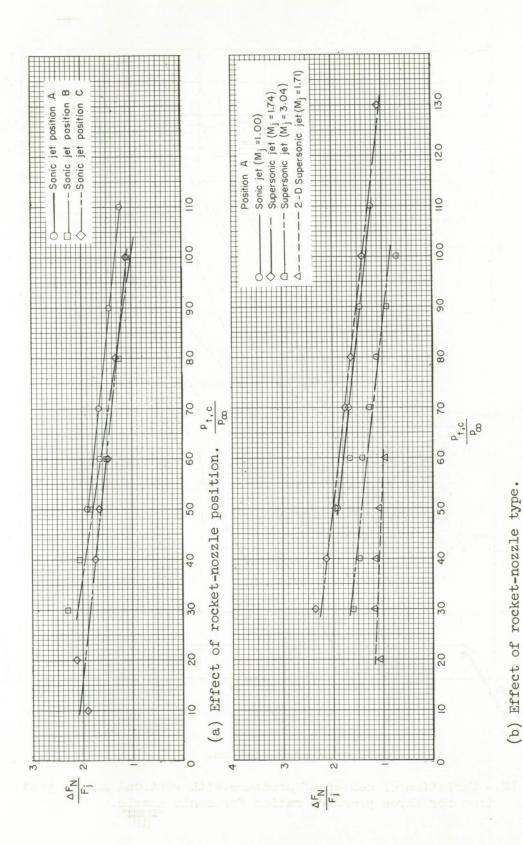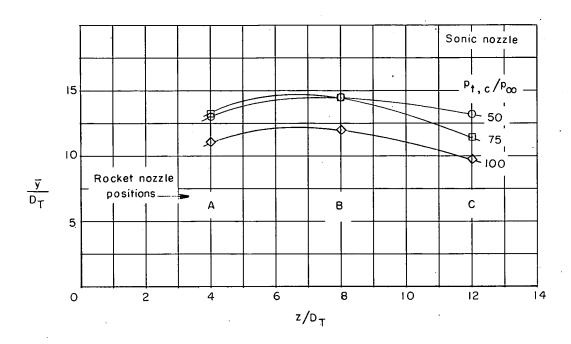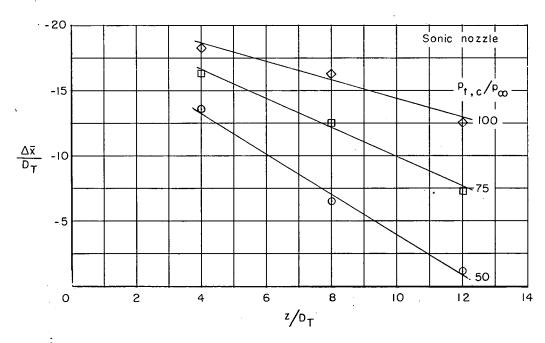
Figure 11.- Ratio of incremental normal force to rocket thrust as a function of pressure ratio for various nozzle positions and nozzle types.

(a) Spanwise variation.

(b) Chordwise variation.

Figure 12.- Variation of center of pressure with vertical nozzle posi-
tion for three pressure ratios for sonic nozzle.
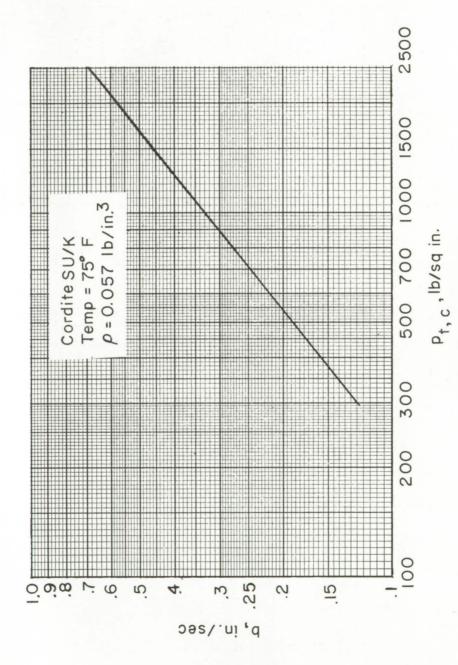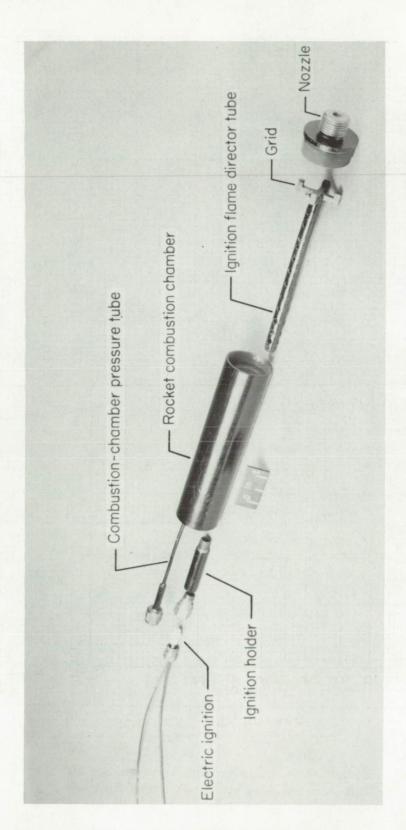
Figure 13.- Burning rate as a function of combustion-chamber pressure.

Figure 14.- Rocket components used in the investigation. L-57-3208.1
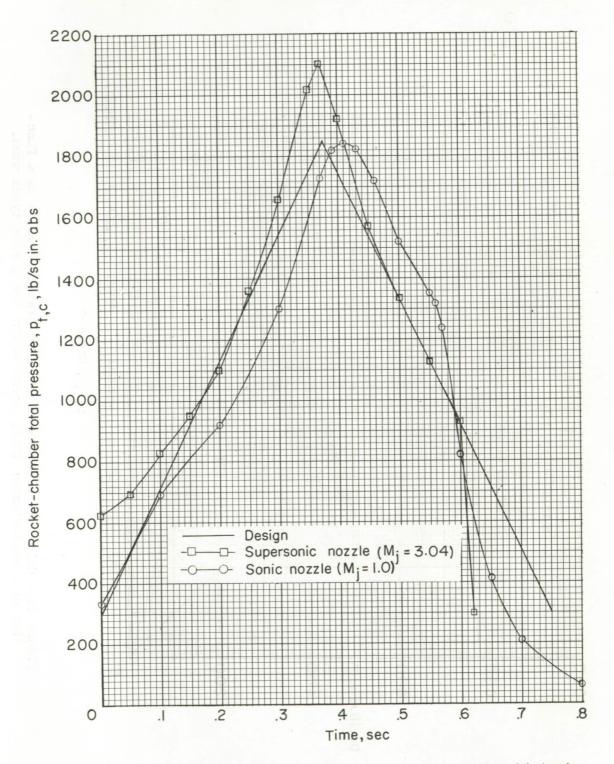
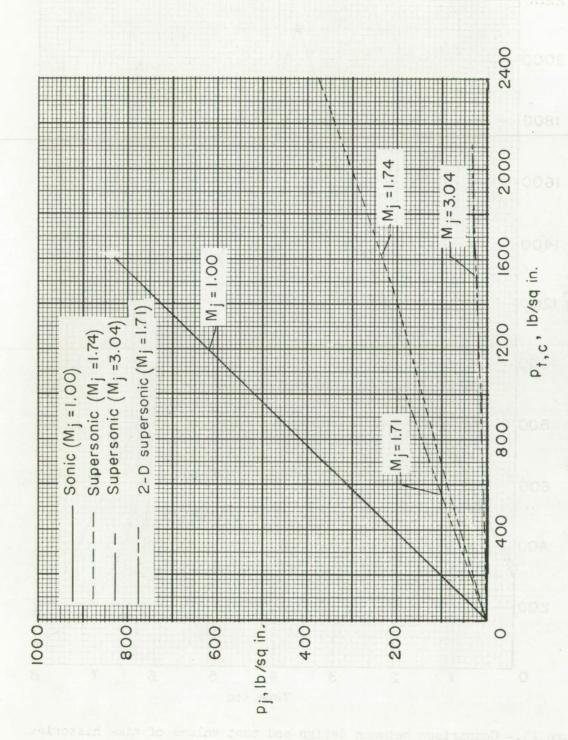Figure 15.- Comparison between design and test values of time histories of rocket-chamber total pressure.

Figure 16.- Calibration curves of jet-exit static pressure as a function of rocket-chamber total pressure for the nozzle types used.